Enhanced mGlu5 Signaling in Excitatory Neurons Promotes Rapid Antidepressant Effects via AMPA Receptor Activation

Holz, Amrei; Muelsch, Felix; Schwarz, Martin K.; Hollmann, Michael; Doebroessy, Mate D.; Coenen, Volker A.; Bartos, Marlene; Normann, Claus; Biber, Knut; van Calker, Dietrich

Published in:
Neuron

DOI:
10.1016/j.neuron.2019.07.011

Article

Neuron

Enhanced mGlu5 Signaling in Excitatory Neurons Promotes Rapid Antidepressant Effects via AMPA Receptor Activation

Graphical Abstract

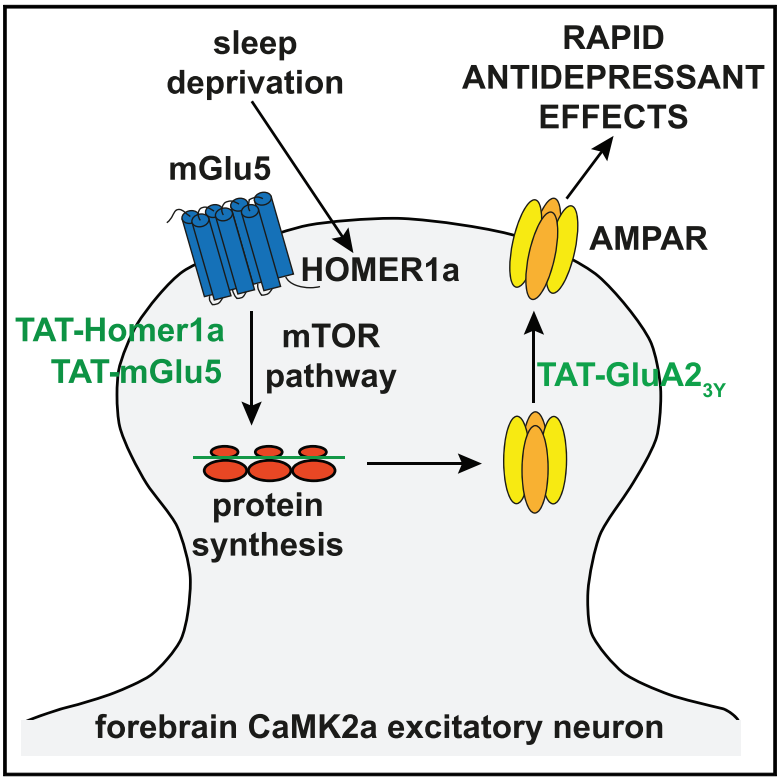

Highlights

- Cell-membrane-permeable TAT-Homer1a elicits rapid antidepressant effects
- SD and TAT-Homer1a activate mGlu5-mTOR signaling and increase AMPAR function
- Antidepressant action of SD requires mGlu5 in excitatory neurons and AMPAR activity
- Modulation of mGlu5 and AMPAR via TAT peptides promotes fast antidepressant effect

Authors

Amrei Holz, Felix Mülsch, Martin K. Schwarz, ..., Knut Biber, Dietrich van Calker, Tsvetan Serchov

Correspondence

tsvetan.serchov@uniklinik-freiburg.de

In Brief

Conventional antidepressants have limited efficacy and many side effects, highlighting the need for fast-acting and specific medications. Holz et al. utilize cell-membrane-permeable TAT-fused peptides, which specifically modulate glutamatergic neurotransmission, as a novel strategy for rapid and effective antidepressant treatment.

Holz et al., 2019, Neuron *104*, 338–352
October 23, 2019
https://doi.org/10.1016/j.neuron.2019.07.011

CellPress

CellPress

Neuron
Article

Enhanced mGlu5 Signaling in Excitatory Neurons Promotes Rapid Antidepressant Effects via AMPA Receptor Activation

Amrei Holz,[1,2] Felix Mülsch,[1] Martin K. Schwarz,[3] Michael Hollmann,[4] Mate D. Döbrössy,[5] Volker A. Coenen,[5] Marlene Bartos,[6] Claus Normann,[1] Knut Biber,[1,7] Dietrich van Calker,[1] and Tsvetan Serchov[5,1,8,*]

[1]Department for Psychiatry and Psychotherapy, Medical Center - University of Freiburg, Faculty of Medicine, University of Freiburg, Hauptstrasse 5, 79104 Freiburg, Germany

[2]Faculty of Biology, University of Freiburg, Schaenzlestrasse 1, 79104 Freiburg, Germany

[3]Functional Neuroconnectomics Group, Department of Experimental Epileptology and Cognition Research, Life and Brain Centre, University of Bonn, 53105 Bonn, Germany

[4]Department of Biochemistry I - Receptor Biochemistry, Faculty of Chemistry and Biochemistry, Ruhr University Bochum, NC6/170, Universitaetsstr. 150, 44801 Bochum, Germany

[5]Department of Stereotactic and Functional Neurosurgery, Medical Center - University Freiburg, Faculty of Medicine, University of Freiburg, Breisacher Str. 64, 79106 Freiburg, Germany

[6]Institute of Physiology I, Systemic and Cellular Neurophysiology, University of Freiburg, Hermann-Herder-Str. 7, 79104 Freiburg, Germany

[7]Department of Neuroscience, Section Medical Physiology, University Medical Center Groningen, 9713 AV Groningen, the Netherlands

[8]Lead Contact

*Correspondence: tsvetan.serchov@uniklinik-freiburg.de

https://doi.org/10.1016/j.neuron.2019.07.011

SUMMARY

Conventional antidepressants have limited efficacy and many side effects, highlighting the need for fast-acting and specific medications. Induction of the synaptic protein Homer1a mediates the effects of different antidepressant treatments, including the rapid action of ketamine and sleep deprivation (SD). We show here that mimicking Homer1a upregulation via intravenous injection of cell-membrane-permeable TAT-Homer1a elicits rapid antidepressant effects in various tests. Similar to ketamine and SD, *in vitro* and *in vivo* application of TAT-Homer1a enhances mGlu5 signaling, resulting in increased mTOR pathway phosphorylation, and upregulates synaptic AMPA receptor expression and activity. The antidepressant action of SD and Homer1a induction depends on mGlu5 activation specifically in excitatory CaMK2a neurons and requires enhanced AMPA receptor activity, translation, and trafficking. Moreover, our data demonstrate a pronounced therapeutic potential of different TAT-fused peptides that directly modulate mGlu5 and AMPA receptor activity and thus might provide a novel strategy for rapid and effective antidepressant treatment.

INTRODUCTION

Major depressive disorder is a highly prevalent disease, associated with high individual suffering, an increased risk for suicide, and a considerable economic burden for the society (Mrazek et al., 2014). Despite their benefits, widely used monoamine-based antidepressant drugs require weeks to months to improve symptoms, have low response rates, and often cause side effects (Trivedi et al., 2006). Even the promising and fast-acting antidepressant treatments of sleep deprivation (SD) and low-dose ketamine have some drawbacks, such as short duration of effects and psychotomimetic side effects (Berman et al., 2000; Dallaspezia and Benedetti, 2015). In spite of many hypotheses, a consistent concept of the complex neurobiology of depression is missing, and the mode of action of the different antidepressant measures, especially those with rapid onset, is not well understood (Duman et al., 2016). Thus, a better understanding of the underlying mechanisms is needed to identify targets for novel drugs with rapid and effective antidepressant action.

Within the last decade, the glutamatergic system has been implicated in the neurobiology and treatment of depression (Duman et al., 2016; Freudenberg et al., 2015; Krystal et al., 2010; van Calker et al., 2018). As key molecules at the postsynaptic density (PSD), Homer proteins form a polymeric network structure and regulate the function of glutamate receptors (Ango et al., 2001; Brakeman et al., 1997; Kammermeier and Worley, 2007; Tu et al., 1998; Xiao et al., 1998). Constitutively expressed long Homers, like Homer1b/c, possess a ligand-binding EVH1 domain and a coiled-coil (CC) domain for dimerization, which allows them to crosslink various synaptic proteins (Ango et al., 2001; Brakeman et al., 1997; Kammermeier and Worley, 2007; Tu et al., 1998; Xiao et al., 1998). In contrast, the short isoform Homer1a, which is rapidly induced by neuronal activity (Brakeman et al., 1997; Kato et al., 1997), lacks the CC domain and interferes with the crosslinking capability of long Homers in a competitive manner (Kammermeier and Worley, 2007; Tu et al., 1998; Xiao et al., 1998). Recently, we have shown that the induction of Homer1a is a common mechanism of action of several antidepressant measures, including rapid-acting SD

and ketamine (Serchov et al., 2015), suggesting a general importance of Homer1a for antidepressant therapy (Serchov et al., 2015, 2016).

However, how Homer1a mediates its antidepressant effects is still unknown. Here, we mimicked the rapid effects of increased Homer1a expression by application of Homer1a fused to the protein transduction domain (TAT), which allows cell membrane permeability and protein delivery into brain neurons passing the blood-brain barrier (Mansouri et al., 2015; Schwarze et al., 1999). *In vivo* intravenous (i.v.) injection of TAT-Homer1a elicits fast and specific antidepressant effects in several test paradigms. *In vitro* and *in vivo* application of TAT-Homer1a uncouples metabotropic glutamate receptor 5 (mGlu5) from its downstream targets, enhances mGlu5 signaling resulting in increased mammalian target of rapamycin (mTOR) pathway activation, and upregulates synaptic α-amino-3-hydroxy-5-methyl-4-isoxazolepropionic acid receptor (AMPAR) expression and activity. Utilizing conditional mGlu5 knockout mice and specific modulation of AMPAR trafficking and function, we show for the first time that the antidepressant effects of SD and Homer1a induction are mediated by mGlu5 in forebrain excitatory neurons and depend on AMPAR synaptic expression and activity. In addition, our data demonstrate that peripheral application of TAT fusion peptides, which specifically modulate mGlu5 signaling and/or synaptic AMPAR synaptic distribution and activity, has rapid antidepressant effects and might provide a novel and effective option for treatment of depression.

RESULTS

Intravenous Injection of TAT-Homer1a Elicits Rapid Antidepressant Effects

In order to directly mimic the rapid induction of Homer1a, we generated cell-permeable TAT-Homer1a fusion proteins, consisting of the coding sequence of mouse Homer1a fused to the cell membrane transduction domain TAT of the human immunodeficiency virus 1, which allows blood-brain barrier and cell membrane permeability and thus successful protein delivery in brain neurons (Figures S1A–S1C) (Mansouri et al., 2015; Schwarze et al., 1999). i.v. application of TAT-Homer1a led to rapid and transient 1.5-fold upregulation of Homer1a expression in the medial prefrontal cortex (mPFC) (Figures S1A and S1B). As controls we used the unconjugated TAT peptide and mutated TAT-H1aW24A, a ligand-binding inactive form of Homer1a (Figures 1A and S1C). TAT-Homer1a decreased immobility time of naive male mice 1 h after i.v. injection in the two basic tests for depressive-like behavior—tail suspension test (TST) (Figures 1B and S1G) and forced swim test (FST) (Figures 1C, S1H, and S1I)—similarly to the rapid effects of ketamine (Figures S1G and S1H). In contrast, the general locomotor and exploratory activity (Figure 1D), as well as the anxiety-like behavior in open field, light-dark transition and elevated plus maze test, were not significantly affected (Figures S1D–S1F).

Then, we investigated the effects of TAT-Homer1a in the chronic behavioral despair mouse model of depression (CDM) (for experimental design, see STAR Methods and Figure 1E) (Normann et al., 2018; Serchov et al., 2015; Sun et al., 2011). Various antidepressant treatments, including acute ketamine, significantly reduced the immobility time during TST and test phase of CDM (Serchov et al., 2015) (Figures S1K and S1L) and rapidly reversed the anhedonic phenotype (Figure S1J), demonstrating the predictive validity of this model. Consistently, a single i.v. injection of TAT-Homer1a evoked a fast antidepressant effect up to 4 h after the application in TST and test phase of CDM in male mice (Figures 1F, 1G, S1K, and S1L). Furthermore, TAT-Homer1a significantly increased the sucrose preference of CDM females in the nose-poke sucrose preference test (SPT) (Figure 1H), a paradigm for automated measurement of reward behavior with gradually increasing effort to reach the sucrose solution, performed in IntelliCage (for experimental design, see STAR Methods) (Alboni et al., 2017).

TAT-Homer1a Uncouples mGlu5 from Its Downstream Calcium Signaling Targets and Induces Agonist-Independent mGlu5 Activation, Resulting in Enhanced mTOR Pathway Signaling

Looking for a potential mechanism, mediating the antidepressant effects of Homer1a, we focused on the interaction between Homer1a and mGlu5, which is the most prominent binding partner of Homer proteins (Brakeman et al., 1997; Kammermeier and Worley, 2007; Xiao et al., 1998). Co-immunoprecipitation experiments revealed that *in vitro* application of TAT-Homer1a on acute brain slices, as well as *in vivo* i.v. injection, significantly decreased Homer1b/c binding to mGlu5 in mPFC (Figures 2A, 2B, S1C, S2A, S2B, and S2M). The long Homer scaffolds crosslink metabotropic glutamate receptors with many proteins involved in calcium signaling, and thus, disruption of mGlu5-Homer1b/c interactions modulates their activity (Ango et al., 2001; Fagni et al., 2000; Ronesi et al., 2012; Tu et al., 1998). Indeed, calcium imaging in the mPFC of Fura-2-loaded acute slices showed that TAT-Homer1a decreased the calcium responses evoked by bath application of mGlu1/5 agonist (RS)-3,5-dihydroxyphenylglycine (DHPG) (Figures S2C–S2E). We extended our measurements using adult Thy1-GCaMP6f transgenic mice, expressing genetically encoded calcium indicator GCaMP6f under control of the neuronal Thy1 promoter (Dana et al., 2014). The TAT-Homer1a-mediated reduction of mGlu1/5-induced calcium signaling was also observed in the mPFC of *ex vivo* recorded slices from i.v.-injected GCaMP6f mice (Figures 2C–2E). These results demonstrate that TAT-Homer1a disrupts mGlu5-Homer1b/c interactions and uncouples mGlu5 from its calcium signaling targets (Figure 2L).

Disrupted mGlu5-Homer1b/c interactions result in a constitutive or agonist-independent mGlu5 activity (Ango et al., 2001; Guo et al., 2016). We found enhanced phosphorylation of Akt, mTOR, and S6 kinase (S6K), but not of extracellular signal-regulated kinases 1/2 (ERK1/2) in acute slices incubated with TAT-Homer1a (Figures 2F–2H and S2F–S2H). This effect was blocked completely by pretreatment with the mGlu5-negative allosteric modulator 2-methyl-6-(phenylethynyl)pyridine hydrochloride (MPEP), indicating that mGlu5 activation is involved in the TAT-Homer1a-mediated induction of the mTOR cascade (Figures 2F–2H). Similarly, we found increased phosphorylation of mTOR and S6K in the mPFC of *in vivo* TAT-Homer1a-injected mice (Figures 2I–2J and S2M), as well as after adenovirus (AAV)-mediated Homer1a overexpression in the mPFC

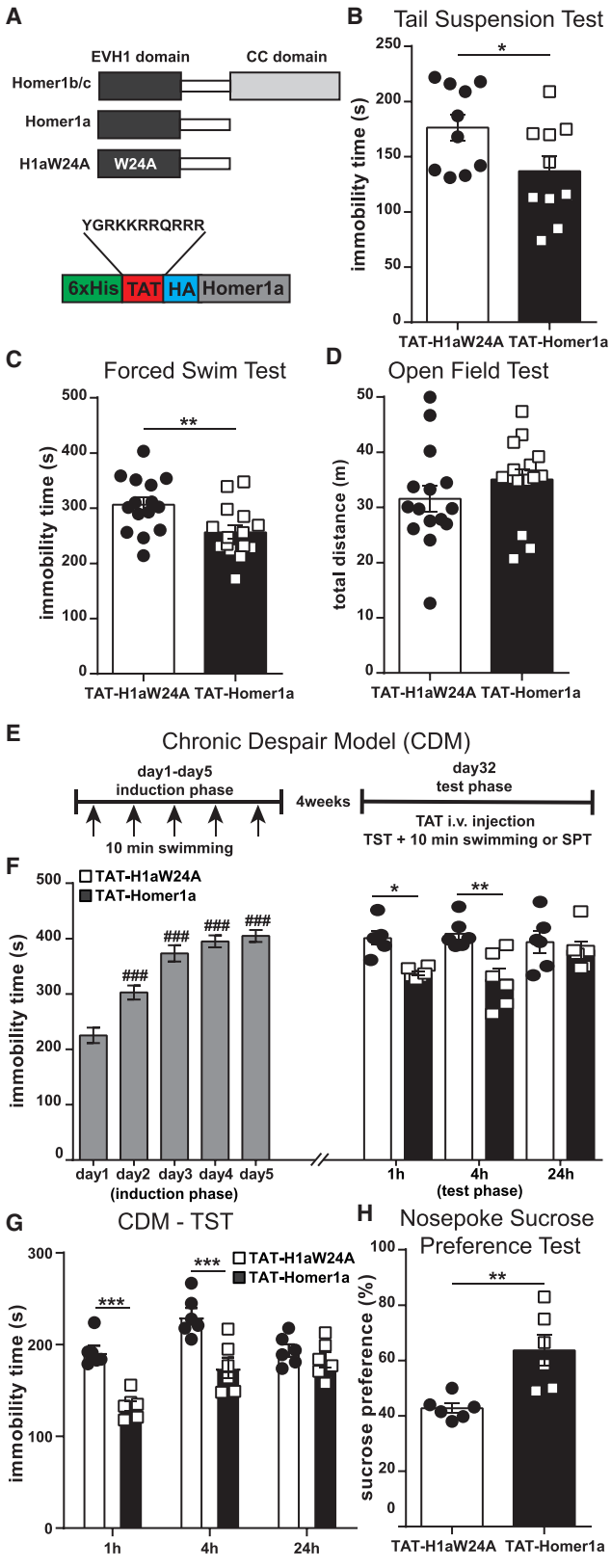

Figure 1. Intravenous Injection of TAT-Homer1a Elicits Rapid Antidepressant Effects

(A) Homer1 domain structure (top) and the TAT-Homer1a fusion protein (bottom): 6xHis, polyhistidine tag; TAT, the arginine-enriched cell membrane transduction domain of HIV-1; HA, hemagglutinin tag.

(B) Immobility time in tail suspension test (TST) 1 h after i.v. injection of 8 mg/kg active TAT-Homer1a or control mutated TAT-H1aW24A (n = 10, Student's t test: *p = 0.0462).

(C) Immobility time in forced swim test (FST) 1 h after injection (n = 10, Student's t test: **p = 0.0084).

(D) Total distance traveled in open field test 1 h after injection (n = 15, Student's t test: p = 0.2646).

(E) Experimental design of the chronic despair model (CDM). The mice were despaired by 10 min swimming for 5 days (induction phase). On day 32, the mice were i.v. injected, followed by TST, and the last 10 min swim session (test phase) was performed 1 h, 4 h, or 24 h after injection or sucrose preference test (SPT).

(F) Immobility time in the induction (n = 36) and test phase (n = 6) of CDM (two-way ANOVA, Bonferroni post hoc test: *p < 0.05, **p < 0.01, $^{###}$p < 0.001 in comparison to day 1).

(G) Immobility time in TST during the test phase of CDM (n = 6, two-way ANOVA, Bonferroni post hoc test: ***p < 0.001).

(H) Nose-poke sucrose preference measured for 12 h following i.v. injection in CDM mice (n = 6, Student's t test: **p = 0.005).

Data are expressed as mean ± SEM, and the individual data points are depicted.

See also Figure S1 and Table S1.

(Figures S2N–S2Q). The mGlu1/5 agonist DHPG increased Akt, mTOR, and S6K phosphorylation in control slices incubated with TAT-H1aW24A but had no effect on TAT-Homer1a-treated slices, where the mTOR cascade was already enhanced (Figures S2I–S2L). Taken together, our data suggest that Homer1a causes constitutive agonist-independent activation of mGlu5 signaling resulting in enhanced mTOR pathway phosphorylation.

The Antidepressant Effect of Sleep Deprivation Is Mediated by mGlu5 Specifically in Forebrain Excitatory CaMK2a Neurons

Since TAT-Homer1a increases mGlu5 activity, we checked whether the fast-acting antidepressant treatments SD and ketamine, which also upregulate Homer1a (Figure S3D) (Serchov et al., 2015), modulate mGlu5 signaling. We found decreased synaptic mGlu5 expression and mTOR phosphorylation in the mPFC of CDM mice, while 6 h of SD or acute ketamine treatment led to increased mGlu5 levels and mTOR phosphorylation (Figures 3A–3C). Moreover, specific siRNA knockdown of Homer1a in the mPFC abolished SD- and ketamine-induced upregulation of mGlu5 in this region, indicating that the mGlu5 increase is mediated by Homer1a induction (Figure 3C). In summary, these findings suggest that mGlu5 might be essential for the antidepressant action of SD and ketamine. To investigate this hypothesis, we used male transgenic mice with an inducible mGlu5 knockout specifically in calcium/calmodulin-dependent protein kinase II alpha (CaMK2a) neurons (CaMK2aCreERT2-mGlu5fl) (Figure 3D). In order to avoid developmental artifacts, the conditional mGlu5 deletion was induced during adulthood by tamoxifen (Figure 3E). mGlu5 ablation did not affect general locomotor activity, anxiety- and depression-like behavior, the induction of chronic behavioral despair in CDM, or SD- and ketamine-mediated upregulation of Homer1a (Figures S3A–S3D). However, the

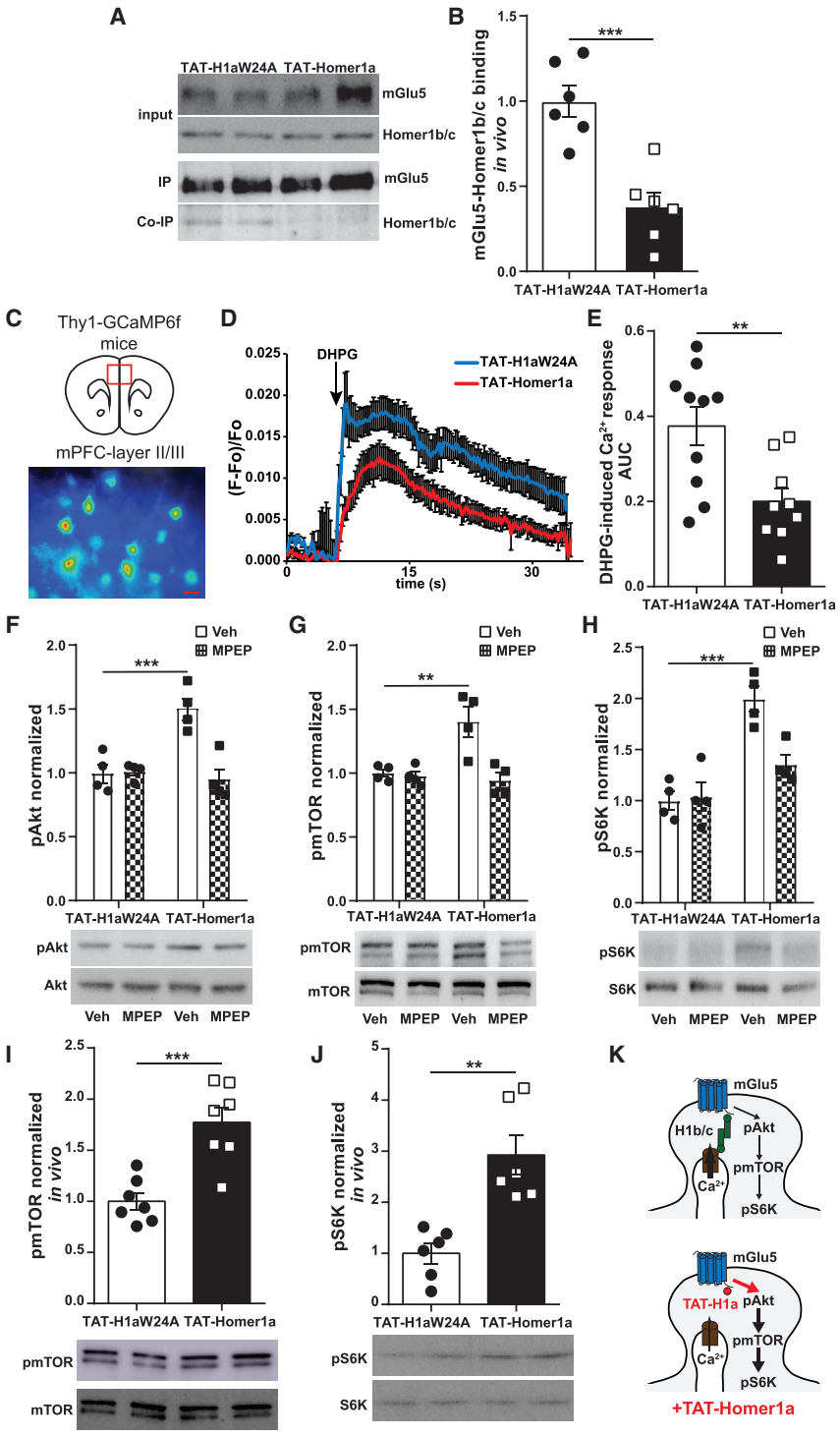

Figure 2. TAT-Homer1a Uncouples mGlu5 from Its Downstream Calcium Effectors and Induces Enhanced mGlu5 Signaling toward mTOR Pathway

(A and B) Representative western blot (A) and quantitative data of mGlu5-Homer1b/c binding normalized to input (B) in the mPFC of CDM mice 1 h after i.v. injection of 8 mg/kg TAT-H1aW24A/Homer1a (Student's t test, n = 6, ***p = 0.0006).

(C) *Ex vivo* GCaMP6f fluorescence in layer II-III pyramidal cells of an acute mPFC slice from an adult Thy1-GCaMP6f mouse (scale bar, 25 μm).

(D and E) Average ΔF showing peak calcium responses (D) and average integrated calcium responses calculated as the area under the curve (AUC) (E) to 100 nM DHPG in the mPFC of Thy1-GCaMP6f CDM mice i.v. injected with TAT-H1aW24A/Homer1a (n = 9, 10 slices (average of 15–25 cells per slice) from 3–4 mice per group; Student's t test: **p = 0.0063).

(F–H) Representative western blot (bottom) and quantitative data (top) of pAkt (F), pmTOR (G), and pS6K (H) levels in acute brain slices treated for 1 h with 100 nM TAT-H1aW24A/Homer1a and 10 μM MPEP or DMSO (Veh) (n = 4, two-way ANOVA, Bonferroni post hoc test: **p < 0.01, ***p < 0.001).

(I and J) Representative western blots (bottom) and quantitative data (top) of pmTOR (I) and pS6K (J) levels in the mPFC of CDM mice 1 h after i.v. injection of 8 mg/kg TAT-H1aW24A/Homer1a (Student's t test: I: n = 7, ***p = 0.0005; J: n = 6, **p = 0.0014).

(K) Model of TAT-Homer1a-induced effects on mGlu5 signaling.

Data are expressed as mean ± SEM, and the individual data points are depicted.

See also Figure S2 and Table S1.

Enhancement of mGlu5 Signaling by TAT-mGlu5 Specifically in CaMK2a Neurons Mimics the Rapid Antidepressant Effects of Homer1a

To investigate directly the role of mGlu5 in mouse depression-like behavior, we used a TAT-mGlu5act decoy peptide that contains the Homer binding site of mGlu5 (ALTPPSPFR). It has a shorter size than TAT-Homer1a, allowing better cell permeability (Ronesi et al., 2012; Ronesi and Huber, 2008; Tronson et al., 2010). TAT-mGlu5act application increased mGlu5 expression and mTOR phosphorylation *in vivo* in mPFC (Figures 4A, 4B, and S4A) and uncoupled mGlu5 from its downstream calcium signaling *in vitro* in acute mPFC slices (Figures S4B and S4C), mimicking the effects of Homer1a. As control we used the mutated TAT-mGlu5mut (ALTPLSPRR) unable to bind to the EVH1 domain (Ronesi et al., 2012; Ronesi and Huber, 2008; Tronson et al., 2010). TAT-mGlu5act i.v. injection decreased the immobility time in TST (Figure 4C) and FST (Figure 4D) without any significant effect on general locomotor activity and deletion of mGlu5 in CaMK2a neurons abolished the antidepressant effects of 6 h SD in CDM mice (Figures 3F and 3G). In contrast, it did not influence the effects of ketamine (Figures 3H and 3I). Taken together, these data point toward a general importance of mGlu5, specifically in forebrain excitatory neurons, for the rapid antidepressant action of SD.

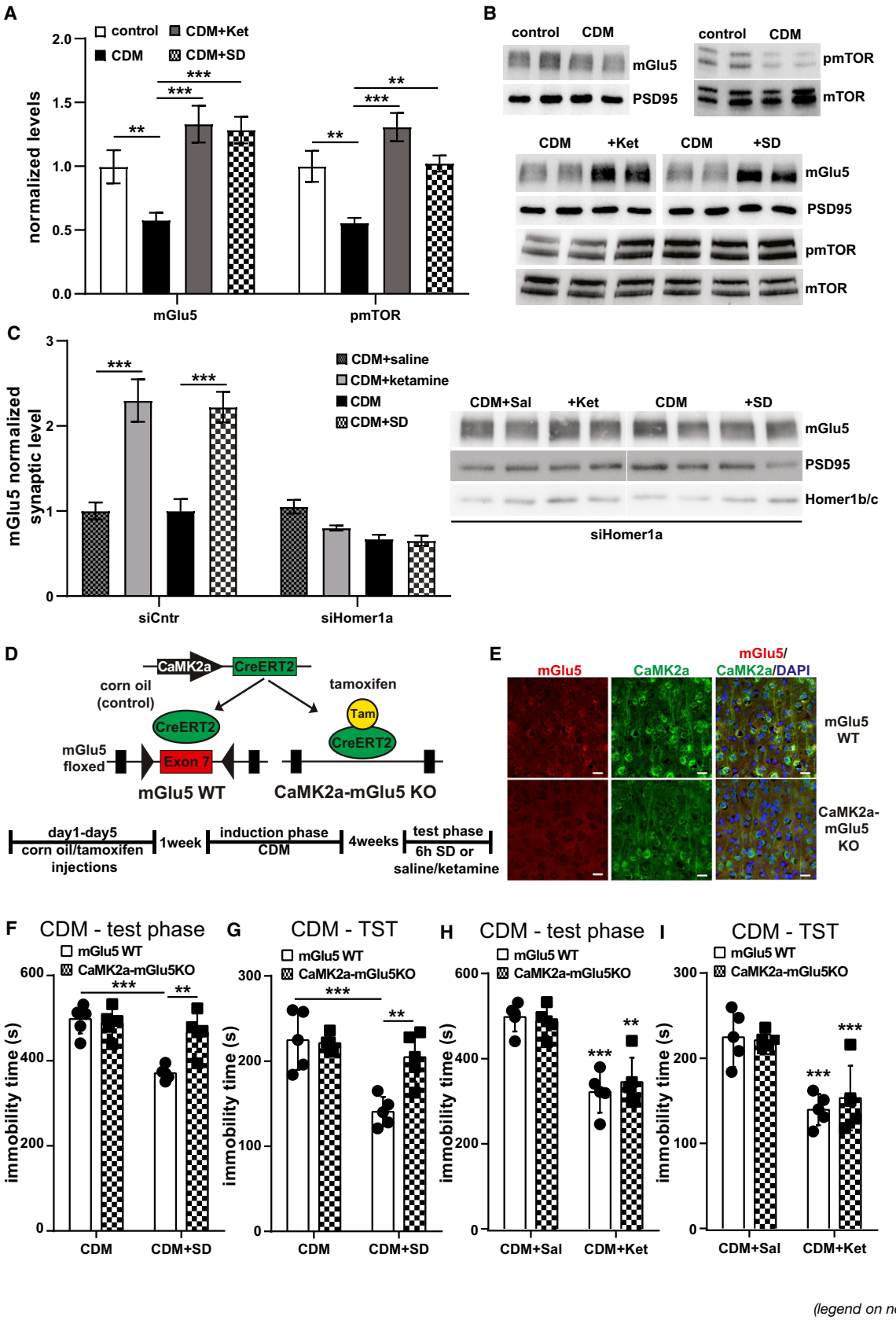

(legend on next page)

anxiety-like behavior (Figure S4D) in control male mice. Moreover, TAT-mGlu5act had more pronounced and persistent (up to 24 h) antidepressant effects in TST (Figure 4F) and test phase (Figure 4E) in CDM male mice than TAT-Homer1a and also increased the sucrose preference in nose-poke SPT in females (Figure 4G). Since enhanced mGlu5 and mTOR signaling are associated with upregulated translation initiation and elongation (Guo et al., 2016; Ronesi and Huber, 2008), we examined whether mGlu5-induced behavioral effects are mediated by increased protein synthesis, similarly to the rapid actions of ketamine (Autry et al., 2011). Thus, we inhibited the protein synthesis with anisomycin prior to TAT-mGlu5act application, which attenuated mGlu5 upregulation (Figure S4E) and blocked the antidepressant effects of TAT-mGlu5act in CDM mice (Figures 4H and 4I). TAT-mGlu5act administration had no significant effects in TST (Figure 4K) and CDM test phase (Figure 4J) of CaMK2a-mGlu5KO animals, indicating that its effects on depression-like behavior are mediated by mGlu5 specifically in forebrain excitatory CaMK2a neurons.

Enhanced mGlu5 Activity Increases the Synaptic Expression and Activity of AMPAR

Considering the potential mechanism mediating the antidepressant effects of enhanced mGlu5 signaling, we hypothesized a role of AMPARs, since they are dynamically regulated by mGlu5 and implicated in the treatment of depression (Diering et al., 2017; Freudenberg et al., 2015; Hu et al., 2010; Maeng et al., 2008). *In vitro* incubation of acute mPFC slices with TAT-Homer1a led to higher synaptic levels of the AMPAR subunit GluA1 (Figure 5A). Moreover, MPEP pretreatment inhibited the effects of TAT-Homer1a on synaptic GluA1 expression, suggesting that GluA1 upregulation is mediated by mGlu5 (Figure 5A). We also checked the effects of TAT-Homer1a on N-methyl-D-aspartate receptor (NMDAR) function *in vitro* in Fura-2-loaded acute mPFC slices. TAT-Homer1a application led to a significant decrease of the NMDA-induced calcium responses, while MPEP pre-incubation abolished these effects, indicating that NMDAR inhibition is mediated by mGlu5 (Figures S5A and S5B).

Furthermore, we found significantly decreased synaptic levels of GluA1 in mPFC of CDM mice compared to controls, whereas SD and acute ketamine application led to elevated synaptic expression of GluA1 in this brain region (Figure 5B). Likewise, i.v. injection of TAT-Homer1a (Figure 5C) or TAT-mGlu5act (Figure 5D), as well as AAV overexpression of Homer1a, upregulated synaptic GluA1 (Figure S6C) in the mPFC of CDM mice. In contrast, specific siRNA knockdown of Homer1a in the mPFC abolishes SD- and ketamine-induced upregulation of GluA1 levels (Figure 5E). We then checked whether mGlu5-induced upregulation of GluA1 is a result of enhanced rates of protein translation. Indeed, we found that pretreatment of TAT-mGlu5act-injected CDM mice with the protein synthesis inhibitor anisomycin completely blocked the mGlu5-mediated increase of GluA1 expression (Figure 5F).

To determine whether the observed changes of synaptic AMPAR expression are accompanied by alterations in the neuronal functionality, we measured AMPA-induced calcium responses in the mPFC. Indeed, *in vitro* incubation of Fura-2-loaded acute slices with TAT-Homer1a resulted in increased calcium responses after bath application of AMPA compared to control TAT-H1aW24A-treated slices (Figures S6A and S6B). In addition, we performed *ex vivo* measurements on acute slices from *in vivo* treated adult Thy1-GCaMP6f transgenic mice. We found significantly decreased AMPA-induced calcium responses in the mPFC of chronically despaired mice in comparison to control non-stressed mice (Figures 5G, S6D, and S6F). In contrast, enhancing the mGlu5 activity via *in vivo* i.v. administration of the TAT-mGlu5act peptide led to a marked increase of AMPA-mediated calcium responses measured 2 h after the injection (Figures 5H, S6E, and S6G).

AMPARs Are Necessary for the Rapid Antidepressant Effects Mediated by Homer1a-mGlu5 Signaling and Sleep Deprivation

To address directly the role of AMPARs in the antidepressant effects of enhanced mGlu5 signaling, we utilized the AMPAR inhibitor 2,3-dioxo-6-nitro-1,2,3,4-tetrahydrobenzo[*f*]quinoxaline-7-sulfonamide (NBQX). Pretreatment with NBQX blocked the antidepressant effects of both TAT-Homer1a (Figures 6A and 6B) and TAT-mGlu5act (Figures 6C and 6D), as well as the rapid action of 6 h SD (Figures 6E and 6F) in TST and test phase of CDM. Moreover, the effects TAT-mGlu5act were also reversed by i.v. application of a TAT-GluA1S845 peptide, which reduces GluA1 phosphorylation at protein kinase A (PKA) site and thus attenuates enhancement of surface and synaptic

Figure 3. The Antidepressant Effects of Sleep Deprivation Are Mediated by mGlu5 Specifically in Forebrain Excitatory CaMK2a Neurons

(A) Synaptic mGlu5 expression and mTOR phosphorylation in the mPFC of control, CDM, CDM mice 24 h after acute treatment with 3 mg/kg ketamine (+Ket), and CDM mice after 6 h SD (+SD) (mGlu5: n = 8, 16, 6, 6; pmTOR n = 6, one-way ANOVA, Bonferroni post hoc test: $^{**}p < 0.01$, $^{***}p < 0.001$).

(B) Representative western blots for (A).

(C) Representative western blot (right) and quantitative data (left) of synaptic mGlu5 expression in the mPFC of CDM, CDM mice 24 h after acute treatment with 3 mg/kg ketamine, and CDM mice after 6 h SD (+SD) stereotaxically bilaterally injected with anti-Homer1a (siHomer1a) or non-target control (siCntr) siRNA into mPFC (n = 4; two-way ANOVA, Bonferroni post hoc test: $^{***}p < 0.001$).

(D) Experimental design: CaMK2aCreERT2-mGlu5fl mice were intraperitoneally (i.p.) injected with 75 mg/kg tamoxifen (CaMK2-mGlu5KO) or corn oil (mGlu5 WT) for 5 days. One week later, the mice were sacrificed for immunohistochemistry or subjected to CDM.

(E) Representative images showing deletion of mGlu5 selectively in CaMK2a neurons (red: anti-mGlu5, green: anti-CaMK2a, blue: DAPI; scale bar, 20 μm).

(F and G) Immobility time in test phase (F) and TST (G) of mGlu5 WT and CaMK2a-mGlu5KO CDM and CDM+6 hSD mice (n = 5, two-way ANOVA, Bonferroni post hoc test: $^{**}p < 0.01$, $^{***}p < 0.001$).

(H and I) Immobility time in test phase (H) and TST (I) performed 24 h after acute i.p. injection of saline (CDM+Sal) or ketamine (CDM+Ket) in mGlu5 WT and CaMK2a-mGlu5KO CDM mice (n = 5, two-way ANOVA, Bonferroni post hoc test: $^{**}p < 0.01$, $^{***}p < 0.001$ in comparison to respective CDM+Sal).

Data are expressed as mean ± SEM, and the individual data points are depicted.

See also Figure S3 and Table S1.

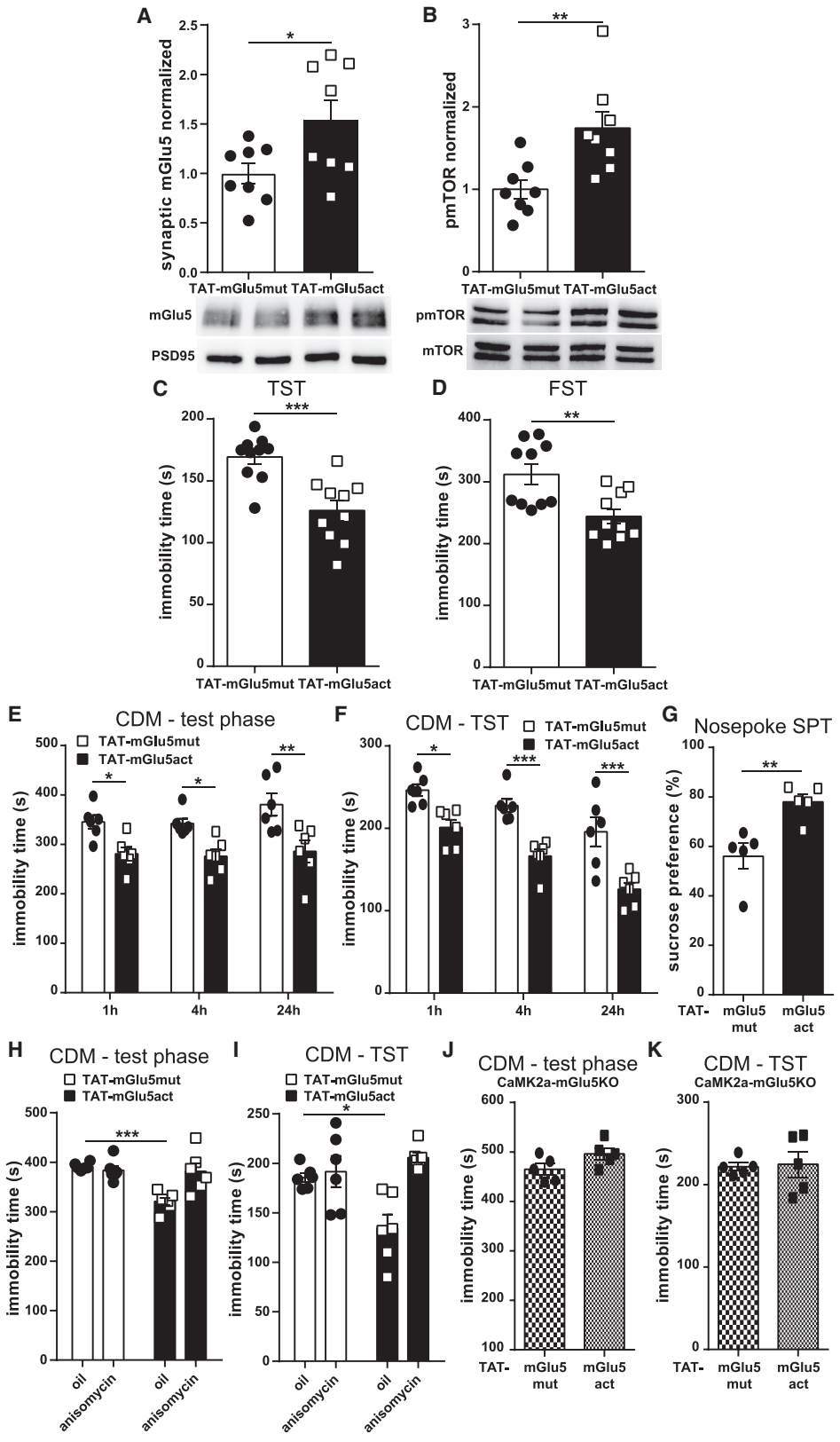

(legend on next page)

expression of AMPARs (Du et al., 2008) (Figures 6G–6I). TAT-GluA1S845 itself did not affect general locomotor activity or anxiety-like behavior (Figure S7C).

Based on these findings, we hypothesized that blocking AMPAR endocytosis with a TAT-GluA2$_{3Y}$ peptide (Figure 6G) (Brebner et al., 2005; Dalton et al., 2008), which results in enhanced AMPAR function (Figures 6A and 6B), has antidepressant effects. Indeed, TAT-GluA2$_{3Y}$-injected naive and CDM male mice showed a decreased immobility time 2 h after injection in FST (Figure 6J) and test phase of CDM (Figure 6K), respectively. However, we found decreased locomotor activity and increased anxiety-like behavior in the open field test (Figure S7C). Taken together, our data demonstrate that upregulation of GluA1, leading to enhanced AMPA-induced calcium responses, is a common final pathway that mediates the rapid antidepressant action of Homer1a induction, mGlu5 activation, and SD.

DISCUSSION

We have previously shown that Homer1a upregulation in the mPFC is a common final pathway mediating the effects of several different antidepressant treatments, including fast-acting SD and ketamine (Serchov et al., 2015), suggesting a general importance of Homer1a for antidepressant therapy (Serchov et al., 2016). Homer1a overexpression mediated by viral or transgenic methods results in a slow and long-lasting increase in Homer1a levels. To date, many studies conducted with TAT-conjugated peptides show promising preclinical evidence demonstrating their ability to cross biological barriers and deliver several types of drugs to their target tissues (Rizzuti et al., 2015). Here, we mimic the fast induction of Homer1a by i.v. injection of TAT-Homer1a, which upregulates Homer1a in mPFC and elicits rapid and specific antidepressant effects, comparable to ketamine and SD (Serchov et al., 2015).

However, little is known about the mechanism how the antidepressant effects of Homer1a are mediated. In general, Homer1a appears to be an important regulator of the activity-induced remodeling of synaptic structures (Inoue et al., 2007) and has been identified as a member of the so-called plasticity-related proteins that promote persistent late-phase synaptic plasticity (Okada et al., 2009). Thus, the rapid induction of Homer1a might provide fast adaptation to stress by modulating synaptic reorganization in neuronal networks involved in mood regulation.

To identify the mechanism of action of Homer1a upregulation, we focused on mGlu5, which is implicated in the pathophysiology and treatment of depression (Krystal et al., 2010). Our data show that TAT-Homer1a disrupts mGlu5 interaction with long Homer variants (Kammermeier and Worley, 2007; Tu et al., 1998) and induces agonist-independent mGlu5 activation (Ango et al., 2001), resulting in enhanced mTOR pathway phosphorylation. Such constitutive mGlu5 signaling toward increased mTOR pathway activation has been previously described in mGlu5$^{R/R}$ transgenic mice, which carry a specific mutation in the Homer binding site of mGlu5, leading to disruption of mGlu5-Homer interactions (Guo et al., 2016). Consistently, the disrupted mGlu5-Homer binding in mGlu5$^{R/R}$ transgenic mice results in an antidepressant phenotype (Guo et al., 2016).

Likewise, we show that synaptic mGlu5 expression and mTOR phosphorylation in mPFC correlate with Homer1a levels and depression-like behavior. Correspondingly, reduced mGlu5 expression and receptor binding has been found in the mPFC of postmortem brains from major depressive disorder patients (Deschwanden et al., 2011), suggesting low mGlu5 neurotransmission in depression. Furthermore, SD and chronic administration of antidepressants result in increased mGlu5 availability in the rodent and human brain (Hefti et al., 2013; Nowak et al., 2014). In addition, targeted pharmacological mGlu5 activation in the nucleus accumbens with the positive allosteric modulator 3-cyano-N-1,3-diphenyl-1H-pyrazol-5-yl)benzamide (CDPPB) promotes resilience to chronic stress (Shin et al., 2015). However, different antagonists of mGlu5 have been proposed as novel agents for the treatment of depression (Hughes et al., 2013). The inconsistencies across these studies could be explained by a recent report showing that both inhibition of mGlu5 in inhibitory neurons and enhanced mGlu5 function in excitatory neurons have antidepressant effects (Lee et al., 2015).

To further test this hypothesis, we generated a knockout mouse with a conditional mGlu5 deletion in CaMK2a forebrain excitatory pyramidal neurons. It has been previously reported that mice with a general mGlu5 deletion exhibit pronounced stress-induced depression-like behavior (Shin et al., 2015) accompanied by several behavioral abnormalities that are not related to depression (Barnes et al., 2015). Moreover, EMX-mGlu5 KO mice, another model of mGlu5 ablation in glutamatergic neurons, show increased depression-like behavior and hyperlocomotor activity (Lee et al., 2015). In contrast,

Figure 4. Intravenous Injection of TAT-mGlu5act Elicits Rapid Antidepressant Effects Mediated by mGlu5 Specifically in Forebrain Excitatory CaMK2a Neurons

(A and B) Representative western blots (bottom) and quantitative data (top) of mGlu5 (A) and pmTOR (B) levels in the mPFC of CDM mice 1 h after i.v. injection of 3 μmol/kg active TAT-mGlu5act or the mutated TAT-mGlu5mut control peptide (Student's t test: n = 8, A: *p = 0.0319; B: **p = 0.0059).

(C) Immobility time in TST 1 h after i.v. injection with 3 μmol/kg TAT-mGlu5act/mut (n = 10, Student's t test: ***p = 0.0004).

(D) Immobility time in FST 1 h after injection (n = 10, Student's t test: **p = 0.0036).

(E) Immobility time in test phase of CDM (n = 6, two-way ANOVA, Bonferroni post hoc test: *p < 0.05, **p < 0.01).

(F) Immobility time in TST of CDM test phase (n = 6, two-way ANOVA, Bonferroni post hoc test: *p < 0.05, ***p < 0.001).

(G) Nose-poke sucrose preference 12 h following i.v. injection of CDM mice (n = 5, Student's t test: **p = 0.0069).

(H and I) Immobility time in test phase (H) and TST (I) of CDM mice 1 h after i.v. injection with 3 μmol/kg TAT-mGlu5mut/act and i.p. injection with 30 mg/kg anisomycin or corn oil 30 min prior to TAT injection (n = 6, two-way ANOVA, Bonferroni post hoc test: *p < 0.05, ***p < 0.001).

(J and K) Immobility time in test phase (J) and TST (K) of CDM CaMK2a-mGlu5KO mice 1 h after i.v. injection of 3 μmol/kg TAT-mGlu5mut/act (n = 5, Student's t test: J: p = 0.0868, K: p = 0.8583).

Data are expressed as mean ± SEM, and the individual data points are depicted.

See also Figure S4 and Table S1.

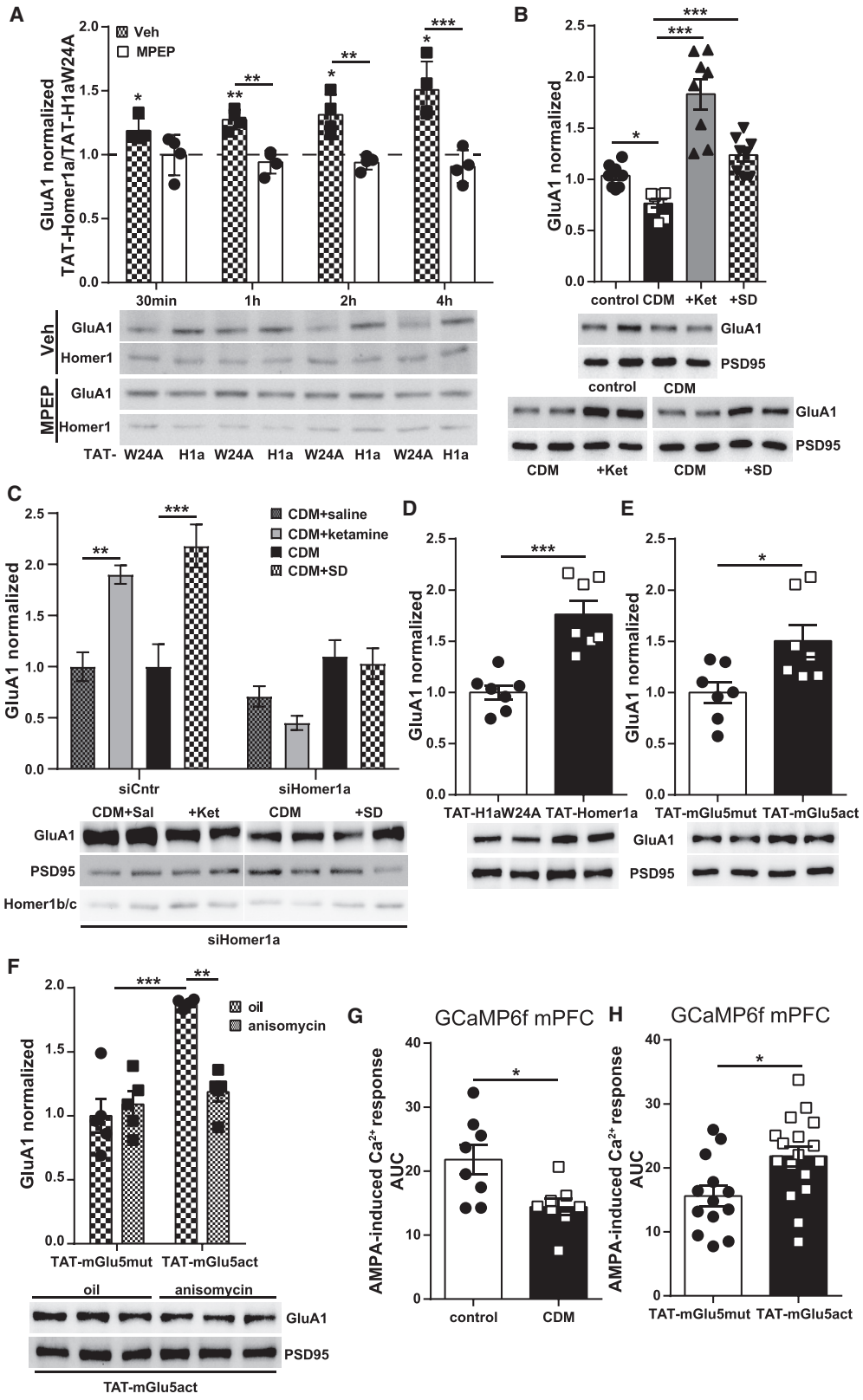

(legend on next page)

CaMK2a-mGlu5 deletion has no effect on general activity or depression- and anxiety-related behavior. Utilizing this mouse model, we show that the antidepressant effects of SD require mGlu5 expression specifically in excitatory CaMK2a neurons. The molecular mechanism of SD is poorly understood, but a potential role of mGlu5 has been suggested (Diering et al., 2017; Hefti et al., 2013; Holst et al., 2017). We have previously shown that the antidepressant effects of SD are mediated by adenosine A_1 receptor-induced upregulation of Homer1a (Serchov et al., 2015). Thus, the modulation of mGlu5 activity by Homer1a might crosslink the adenosinergic and glutamatergic systems in the control of sleep homeostasis and mood.

The mechanism of action of the TAT-mGlu5 peptide has been studied before and is similar to that of Homer1a induction. TAT-mGlu5act disrupts mGlu5-Homer binding (Ronesi et al., 2012; Ronesi and Huber, 2008), decreases mGlu5-mediated calcium responses, and induces agonist-independent activation of mGlu5 signaling toward mTOR pathway phosphorylation and increased translation rates (Ronesi et al., 2012; Tronson et al., 2010). A potential involvement of mTOR signaling in depression has been previously suggested by postmortem studies, which report reduced mTOR and S6K protein levels in the prefrontal cortex of patients with major depressive disorder (Jernigan et al., 2011). Moreover, recent reports indicate that the antidepressant effects of ketamine require mTOR activation and increased protein synthesis (Autry et al., 2011; Li et al., 2010). The enhanced mGlu5-mTOR signaling in general is associated with increased phosphorylation of translation initiation factors and upregulated protein synthesis rates (Guo et al., 2016; Ronesi and Huber, 2008). Likewise, our data demonstrate that the antidepressant effects of the TAT-mGlu5 peptide require protein synthesis, since blocking translation inhibits its action.

To further explore the mechanism underlying the antidepressant action of Homer1a-mGlu5 signaling, we investigated the potential involvement of AMPARs, which are implicated in the mechanism of rapid antidepressant measures (Autry et al., 2011; Freudenberg et al., 2015; Li et al., 2010; Maeng et al., 2008; van Calker et al., 2018). We show that TAT-Homer1a, as well as TAT-mGlu5act, increases synaptic expression of the AMPAR subunit GluA1. Moreover, GluA1 levels and AMPAR functionality in the mPFC correlate with the depression-like behavior. Our findings are supported by previous studies on AMPARs, demonstrating that chronic stress results in decreased total and surface expression of the GluA1 and reduced AMPAR-mediated synaptic currents in the rat prefrontal cortex (Yuen et al., 2012). In postmortem tissues from patients with depression, the mRNA expression of GluA1 in hippocampus and perirhinal cortex is decreased as well (Beneyto et al., 2007; Duric et al., 2013). Conversely, treatment with ketamine induces mTOR-mediated upregulation of synaptic GluA1 expression and increases the amplitude of pyramidal cell excitatory postsynaptic currents in the mPFC of rats (Li et al., 2010). Taken together, both rapid antidepressant measures SD and ketamine might share a common mechanism of action, including Homer1a induction, mTOR pathway activation and potentiation of AMPAR function. Unlike SD, the antidepressant action of ketamine does not require mGlu5 in excitatory neurons, suggesting that the effects of Homer1a are mediated either by a different binding partner than mGlu5, such as compensatory upregulation of the Homer1a-mGlu1 interaction, or by a distinct neuronal cell type. Moreover, a recent report shows ketamine-induced reduction of mGlu5 availability associated with antidepressant response in depressed humans (Esterlis et al., 2018). Thus, further investigations are needed to clarify the role of mGlu5 in the antidepressant action of ketamine.

mGlu5 is also indirectly linked to NMDARs via multimeric protein complexes consisting of Homer1b/c, Shank, PSD95, and the GluN2B subunit. When upregulated, Homer1a disrupts the interaction between mGlu5 and NMDARs, which results in mGlu5-mediated NMDAR inhibition (Bertaso et al., 2010; Moutin et al., 2012; Perroy et al., 2008). Several reports demonstrate that the antidepressant effect of NMDAR blockade depends on increased AMPAR activity (Autry et al., 2011; Koike and Chaki, 2014; Maeng et al., 2008). We similarly show that Homer1a effects require AMPAR activation. However, whether the described Homer1a-mediated inhibition of NMDARs is necessary for increased AMPAR activity and the antidepressant effect of Homer1a is not clear, since a NMDAR inhibition-independent rapid antidepressant action, which also involves sustained activation of AMPARs, has been shown recently (Zanos et al., 2016). Moreover, antidepressant treatments, like ketamine and SD, lead to a strong increase in GluN2B levels, a subunit involved

Figure 5. Enhanced Homer1a and mGlu5 Increase Synaptic Expression and Activity of AMPAR

(A) Synaptic GluA1 AMPAR subunit level in acute brain slices pretreated with DMSO (Veh) or 50 μM MPEP and incubated with 100 nM TAT-H1aW24A or TAT-Homer1a (n = 4 independent experiments, one-sample t test: Veh: 30 min *p = 0.0239, 1 h **p = 0.0058, 2 h *p = 0.0279, 4 h *p = 0.0196; MPEP: 30 min p = 0.3872, 1 h p = 0.2627, 2 h p = 0.2297, 4 h p = 0.3149; two-way ANOVA, Bonferroni post hoc test: Veh versus MPEP: **p < 0.01, ***p < 0.001).

(B) Quantitative data (top) and representative western blot (bottom) of synaptic GluA1 levels in mPFC of control, CDM, CDM mice 24 h after acute treatment with 3 mg/kg ketamine (+Ket), and CDM mice after 6 h SD (+SD) (n = 8, one-way ANOVA, Bonferroni post hoc test: *p < 0.05, ***p < 0.001).

(C) Quantitative data (top) and representative western blot (bottom) of synaptic GluA1 expression in mPFC of CDM mice, CDM mice 24 h after acute treatment with 3 mg/kg ketamine, and CDM mice after 6 h SD (+SD) stereotaxically bilaterally injected with anti-Homer1a (siHomer1a) or non-target control (siCntr) siRNA into mPFC (n = 4; two-way ANOVA, Bonferroni post hoc test: **p < 0.01, ***p < 0.001).

(D and E) Synaptic GluA1 levels in mPFC of CDM mice i.v. injected with 8 mg/kg TAT-H1W24A/Homer1a (D) or 3 μmol/kg TAT-mGlu5mut/act (E) (n = 7, Student's t test D: ***p = 0.0002, E: *p = 0.0199).

(F) Quantitative data (top) and representative western blot (bottom) of synaptic GluA1 levels in mPFC of CDM mice 1 h after i.v. injection with TAT-mGlu5mut/act and i.p. injection of 30 mg/kg anisomycin or control corn oil prior to TAT injection (n = 5, two-way ANOVA, Bonferroni post hoc test: **p < 0.01, ***p < 0.001).

(G and H) Average integrated calcium responses to 5 μM AMPA in mPFC of control and CDM Thy1-GCaMP6f mice (G) (n = 8 slices from 4 mice, Student's t test: *p = 0.0139) and CDM Thy1-GCaMP6f mice 2 h after i.v. injection with TAT-mGlu5act/mut (H) (n = 13, 17 slices from 4 mice, Student's t test: *p = 0.0103).

Data are expressed as mean ± SEM, and the individual data points are depicted.

See also Figures S5 and S6 and Table S1.

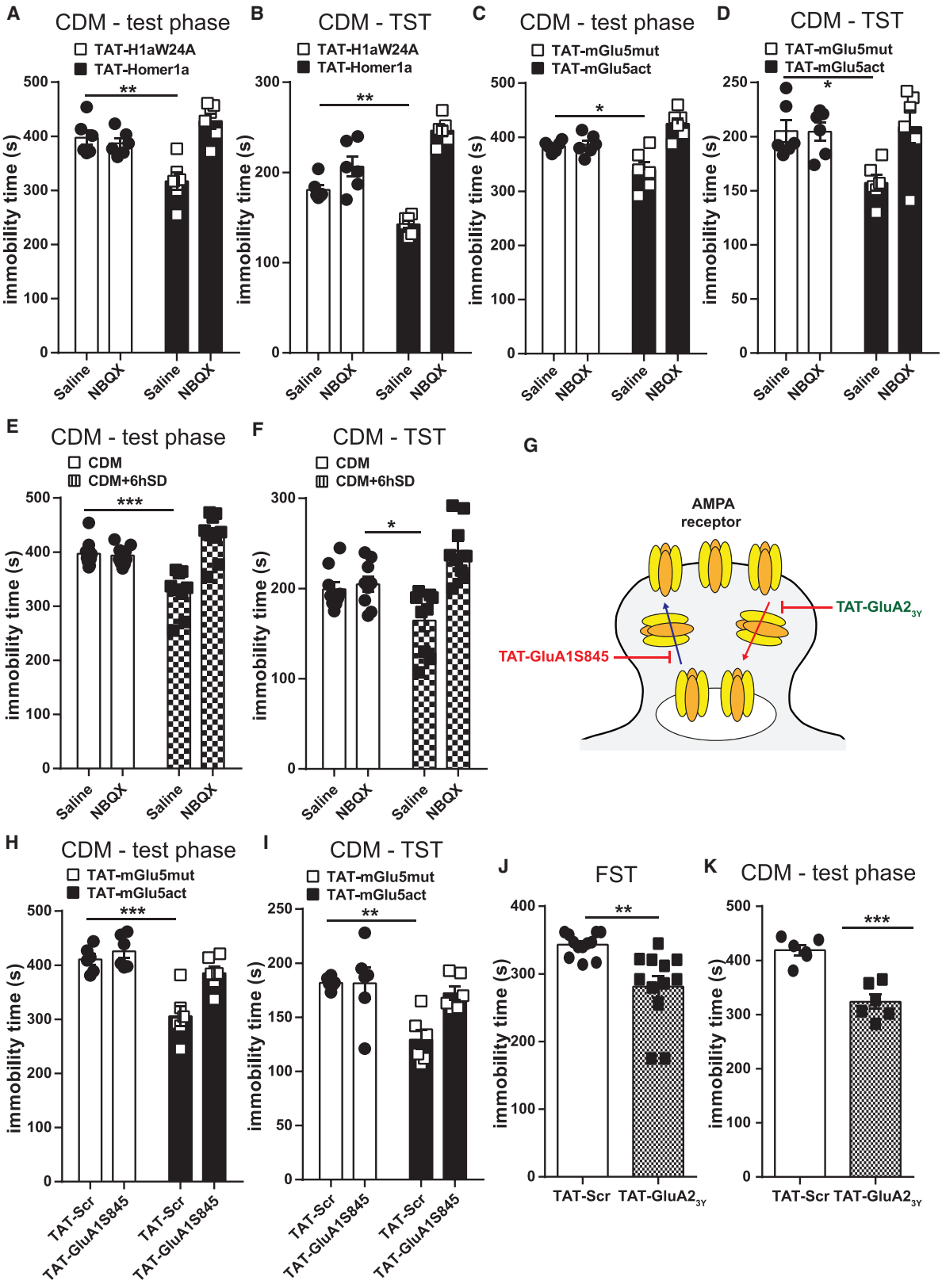

(legend on next page)

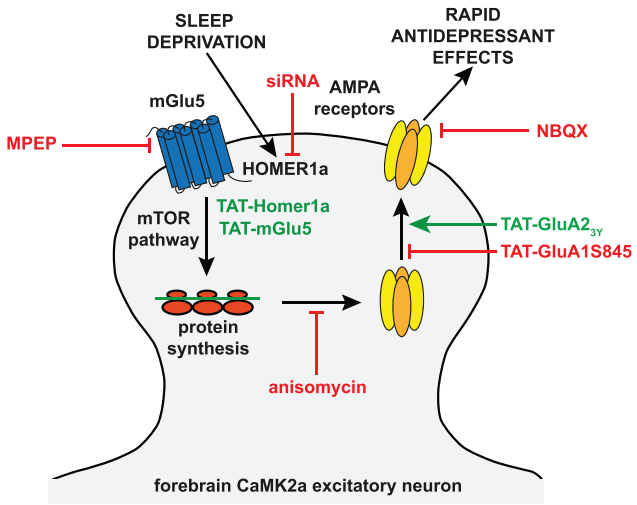

Figure 7. Model

The rapid antidepressant action of SD and Homer1a induction is mediated by mGlu5 activation specifically in excitatory CaMK2a neurons and requires enhanced AMPAR activity, translation, and exocytosis. Homer1a uncouples mGlu5 from long Homer variants, leading to constitutive agonist-independent mGlu5 activation followed by enhanced mTOR signaling that in turn stimulates protein translation. Increased translation rates result in elevated synaptic expression of the AMPAR subunit GluA1 and enhanced AMPAR-mediated synaptic transmission with subsequent antidepressant effects.

in the therapeutic action of NMDAR antagonism (Miller et al., 2014), in the mPFC of CDM mice (Figure S5C).

There is controversial evidence about the direction of AMPAR modulation by Homer1a and mGlu5. Our data demonstrate that increased Homer1a-mGlu5 signaling upregulates AMPAR function via enhanced GluA1 protein translation and trafficking. In contrast, it has been reported that increased Homer1a expression leads to homeostatic downscaling of AMPARs mediated by mGlu5-coupled protein kinase Cγ activation (Diering et al., 2017; Hu et al., 2010). These differential effects of Homer1a/mGlu5 might be explained by the fact that we describe increased expression of AMPARs during wake phase and/or after sleep deprivation, while AMPARs are dynamically scaled down during sleep phase (Diering et al., 2017). Moreover, Homer1a regulates the activity-induced changes of AMPAR surface expression in a biphasic manner (Inoue et al., 2007) and plays a key role during late-phase long-term potentiation, where it amplifies AMPAR function (Hennou et al., 2003; Inoue et al., 2007; Okada et al., 2009).

In summary, our data provide evidence that the rapid antidepressant action of SD and Homer1a induction is mediated by mGlu5 activation specifically in excitatory CaMK2a neurons and requires enhanced AMPAR activity, translation, and trafficking. In brief, SD induces Homer1a, which uncouples mGlu5 from long Homer proteins, leading to constitutive agonist-independent mGlu5 activation followed by enhanced mTOR signaling that in turn stimulates protein translation. Increased translation rates result in elevated synaptic expression of the AMPAR subunit GluA1 and enhanced AMPAR-mediated synaptic transmission in CaMK2a excitatory neurons with subsequent antidepressant effects (Figure 7). How enhanced AMPAR function is linked to the antidepressant phenotype remains to be studied. AMPARs are involved in synaptic plasticity, which is strongly associated with the etiology of depression (van Calker et al., 2018). Long-term synaptic plasticity is dysregulated in animal models of depression and in depressed humans and is in turn corrected by a wide variety of antidepressive interventions (Duman et al., 2016).

In addition, we describe here the therapeutic potential of different TAT-fused peptides as fast-acting antidepressant drugs that modulate glutamatergic neurotransmission. These blood-brain barrier and cell-membrane-permeable peptides allow peripheral administration and have no obvious side effects in behavioral tests with mice. Remarkably, the therapeutic potential of NA-1, a TAT-conjugated peptide that modulates NMDAR function, has already been successfully tested in patients with stroke in a phase 2 clinical trial (Hill et al., 2012). All three TAT proteins/peptides show fast antidepressant effects that persist in case of TAT-mGlu5act for at least 24 h. The TAT-mGlu5 peptide also seems to be the best candidate regarding the balance between efficacy and adverse effects. However, further studies are needed to test side effects, pharmacokinetics, and a possible use in psychiatry. Also, a non-invasive intranasal delivery of the TAT peptides might be considered (Brown and Liu, 2014), which enables more precise brain region targeting to the prefrontal cortex, increases specificity, efficacy, and effectiveness, and might provide new treatment options for patients suffering from depression.

Figure 6. AMPAR Are Necessary for the Rapid Antidepressant Effects Mediated by Homer1a Induction, Enhanced mGlu5 Signaling and Sleep Deprivation

(A and B) Immobility time in test phase (A) and TST (B) of CDM mice 1 h after i.v. injection of 8 mg/kg TAT-H1aW24A/Homer1a and i.p. injection of 10 mg/kg NBQX or saline (vehicle) 30 min before TAT injection (n = 6, two-way ANOVA, Bonferroni post hoc test: $^{**}p < 0.01$).

(C and D) Immobility time in test phase (C) and TST (D) of CDM mice 1 h after i.v. injection with 3 μmol/kg TAT-mGlu5mut/act and i.p. injection with 10 mg/kg NBQX or saline 30 min before TAT injection (n = 6, two-way ANOVA, Bonferroni post hoc test: $^{*}p < 0.05$).

(E and F) Immobility time in test phase (E) and TST (F) of CDM mice after 6 h of sleep deprivation and i.p. injection with 10 mg/kg NBQX or saline 30 min before testing (n = 9, two-way ANOVA, Bonferroni post hoc test: $^{*}p < 0.05$, $^{***}p < 0.001$).

(G) Mechanism of action of the TAT-GluA1S845 and TAT-GluA2$_{3Y}$ peptides.

(H and I) Immobility time in test phase (H) and TST (I) of CDM mice 1 h after the i.v. injection with 3 μmol/kg TAT-mGlu5mut/act and i.v. injection with 3 μmol/kg scrambled control TAT-Scr or active TAT-GluA1S845 (n = 6, two-way ANOVA, Bonferroni post hoc test: $^{**}p < 0.01$, $^{***}p < 0.001$).

(J and K) Immobility time in FST (n = 12) (J) and test phase of CDM (n = 6 mice per group) (K) 2 h after i.v. injections of 1.5 μmol/kg TAT-Scr or TAT-GluA2$_{3Y}$ (Student's t test: I: $^{**}p = 0.0012$, J: $^{***}p = 0.0002$).

Data are expressed as mean ± SEM, and the individual data points are depicted.

See also Figure S7 and Table S1.

STAR★METHODS

Detailed methods are provided in the online version of this paper and include the following:

- KEY RESOURCES TABLE
- LEAD CONTACT AND MATERIALS AVAILABILITY
- EXPERIMENTAL MODEL AND SUBJECT DETAILS
- METHODS DETAILS
  - TAT-Homer1a Fusion Protein Generation, Expression and Purification
  - Drug Treatment
  - Peptide Administration
  - Behavioral Studies
  - Open Field Test
  - Tail Suspension Test
  - Forced Swim Test
  - Light/dark Transition Test
  - Elevated Plus Maze Test
  - Chronic Behavioral Despair Model
  - Behavioral Analysis in the IntelliCage
  - Sleep Deprivation
  - Immunohistochemistry
  - *In vivo* Stereotaxic Microinjections of Recombinant Adeno-Associated Viral Vectors
  - *In vivo* Stereotaxic Microinjections of siRNA
  - Preparation of Acute Brain Slices, *in vitro* Treatment and Fura-2 Calcium Imaging
  - Calcium Imaging with Thy1-GCaMP6f Mice
  - Preparation of Total, Synaptosomal and PSD Fractions
  - Co-immunoprecipitation
  - Western Blot
  - Quantitative Real-time PCR (qRT-PCR)
  - Statistical Analysis
- DATA AND CODE AVAILABILITY

SUPPLEMENTAL INFORMATION

Supplemental Information can be found online at https://doi.org/10.1016/j.neuron.2019.07.011.

ACKNOWLEDGMENTS

We thank Dr. Steven Dowdy for distributing the pTAT-HA expression vector, Dr. Anis Contractor for providing the mGlu5fl mouse line, and Prof. Dr. Norbert Klugbauer for sharing the behavioral lab. The study was funded by a grant from the German Research Council (SE 2666/2-1) and a grant from the Forschungskommission of the Medical Faculty of University of Freiburg (SER1149/17) to T.S. and by the German Ministry for Research and Education (BMBF) grant e:bio – Modul I –ReelinSys (Project B: 0316174A) to K.B.

AUTHOR CONTRIBUTIONS

Conceptualization, T.S., D.v.C., C.N., and K.B.; Methodology, T.S., A.H., F.M., and M.K.S.; Investigation, T.S., A.H., F.M., and M.K.S.; Resources, M.K.S., M.H., M.D.D., V.A.C., M.B., and C.N.; Writing – Original Draft, A.H. and T.S.; Writing – Review and Editing, A.H., T.S., D.v.C., M.H., C.N., and K.B.; Funding Acquisition, T.S. and K.B.; Supervision, T.S., K.B., C.N., and D.v.C.

DECLARATION OF INTERESTS

The authors declare no competing interest.

Received: December 1, 2018
Revised: May 14, 2019
Accepted: July 12, 2019
Published: August 13, 2019

REFERENCES

Alboni, S., van Dijk, R.M., Poggini, S., Milior, G., Perrotta, M., Drenth, T., Brunello, N., Wolfer, D.P., Limatola, C., Amrein, I., et al. (2017). Fluoxetine effects on molecular, cellular and behavioral endophenotypes of depression are driven by the living environment. Mol. Psychiatry *22*, 552–561.

Ango, F., Prézeau, L., Muller, T., Tu, J.C., Xiao, B., Worley, P.F., Pin, J.P., Bockaert, J., and Fagni, L. (2001). Agonist-independent activation of metabotropic glutamate receptors by the intracellular protein Homer. Nature *411*, 962–965.

Autry, A.E., Adachi, M., Nosyreva, E., Na, E.S., Los, M.F., Cheng, P.F., Kavalali, E.T., and Monteggia, L.M. (2011). NMDA receptor blockade at rest triggers rapid behavioural antidepressant responses. Nature *475*, 91–95.

Barnes, S.A., Pinto-Duarte, A., Kappe, A., Zembrzycki, A., Metzler, A., Mukamel, E.A., Lucero, J., Wang, X., Sejnowski, T.J., Markou, A., and Behrens, M.M. (2015). Disruption of mGluR5 in parvalbumin-positive interneurons induces core features of neurodevelopmental disorders. Mol. Psychiatry *20*, 1161–1172.

Becker-Hapak, M., McAllister, S.S., and Dowdy, S.F. (2001). TAT-mediated protein transduction into mammalian cells. Methods *24*, 247–256.

Beneyto, M., Kristiansen, L.V., Oni-Orisan, A., McCullumsmith, R.E., and Meador-Woodruff, J.H. (2007). Abnormal glutamate receptor expression in the medial temporal lobe in schizophrenia and mood disorders. Neuropsychopharmacology *32*, 1888–1902.

Berman, R.M., Cappiello, A., Anand, A., Oren, D.A., Heninger, G.R., Charney, D.S., and Krystal, J.H. (2000). Antidepressant effects of ketamine in depressed patients. Biol. Psychiatry *47*, 351–354.

Bertaso, F., Roussignol, G., Worley, P., Bockaert, J., Fagni, L., and Ango, F. (2010). Homer1a-dependent crosstalk between NMDA and metabotropic glutamate receptors in mouse neurons. PLoS ONE *5*, e9755.

Brakeman, P.R., Lanahan, A.A., O'Brien, R., Roche, K., Barnes, C.A., Huganir, R.L., and Worley, P.F. (1997). Homer: a protein that selectively binds metabotropic glutamate receptors. Nature *386*, 284–288.

Brebner, K., Wong, T.P., Liu, L., Liu, Y., Campsall, P., Gray, S., Phelps, L., Phillips, A.G., and Wang, Y.T. (2005). Nucleus accumbens long-term depression and the expression of behavioral sensitization. Science *310*, 1340–1343.

Brown, V., and Liu, F. (2014). Intranasal delivery of a peptide with antidepressant-like effect. Neuropsychopharmacology *39*, 2131–2141.

Dallaspezia, S., and Benedetti, F. (2015). Sleep deprivation therapy for depression. Curr. Top. Behav. Neurosci. *25*, 483–502.

Dalton, G.L., Wang, Y.T., Floresco, S.B., and Phillips, A.G. (2008). Disruption of AMPA receptor endocytosis impairs the extinction, but not acquisition of learned fear. Neuropsychopharmacology *33*, 2416–2426.

Dana, H., Chen, T.W., Hu, A., Shields, B.C., Guo, C., Looger, L.L., Kim, D.S., and Svoboda, K. (2014). Thy1-GCaMP6 transgenic mice for neuronal population imaging in vivo. PLoS ONE *9*, e108697.

Deschwanden, A., Karolewicz, B., Feyissa, A.M., Treyer, V., Ametamey, S.M., Johayem, A., Burger, C., Auberson, Y.P., Sovago, J., Stockmeier, C.A., et al. (2011). Reduced metabotropic glutamate receptor 5 density in major depression determined by [(11)C]ABP688 PET and postmortem study. Am. J. Psychiatry *168*, 727–734.

Diering, G.H., Nirujogi, R.S., Roth, R.H., Worley, P.F., Pandey, A., and Huganir, R.L. (2017). Homer1a drives homeostatic scaling-down of excitatory synapses during sleep. Science *355*, 511–515.

Du, J., Creson, T.K., Wu, L.J., Ren, M., Gray, N.A., Falke, C., Wei, Y., Wang, Y., Blumenthal, R., Machado-Vieira, R., et al. (2008). The role of hippocampal GluR1 and GluR2 receptors in manic-like behavior. J. Neurosci. *28*, 68–79.

Duman, R.S., Aghajanian, G.K., Sanacora, G., and Krystal, J.H. (2016). Synaptic plasticity and depression: new insights from stress and rapid-acting antidepressants. Nat. Med. *22*, 238–249.

Duric, V., Banasr, M., Stockmeier, C.A., Simen, A.A., Newton, S.S., Overholser, J.C., Jurjus, G.J., Dieter, L., and Duman, R.S. (2013). Altered expression of synapse and glutamate related genes in post-mortem hippocampus of depressed subjects. Int. J. Neuropsychopharmacol. *16*, 69–82.

Esterlis, I., DellaGioia, N., Pietrzak, R.H., Matuskey, D., Nabulsi, N., Abdallah, C.G., Yang, J., Pittenger, C., Sanacora, G., Krystal, J.H., et al. (2018). Ketamine-induced reduction in mGluR5 availability is associated with an antidepressant response: an [^{11}C]ABP688 and PET imaging study in depression. Mol. Psychiatry *23*, 824–832.

Fagni, L., Chavis, P., Ango, F., and Bockaert, J. (2000). Complex interactions between mGluRs, intracellular Ca2+ stores and ion channels in neurons. Trends Neurosci. *23*, 80–88.

Freudenberg, F., Celikel, T., and Reif, A. (2015). The role of α-amino-3-hydroxy-5-methyl-4-isoxazolepropionic acid (AMPA) receptors in depression: central mediators of pathophysiology and antidepressant activity? Neurosci. Biobehav. Rev. *52*, 193–206.

Guo, W., Molinaro, G., Collins, K.A., Hays, S.A., Paylor, R., Worley, P.F., Szumlinski, K.K., and Huber, K.M. (2016). Selective disruption of metabotropic glutamate receptor 5-Homer interactions mimics phenotypes of fragile X syndrome in mice. J. Neurosci. *36*, 2131–2147.

Hefti, K., Holst, S.C., Sovago, J., Bachmann, V., Buck, A., Ametamey, S.M., Scheidegger, M., Berthold, T., Gomez-Mancilla, B., Seifritz, E., and Landolt, H.P. (2013). Increased metabotropic glutamate receptor subtype 5 availability in human brain after one night without sleep. Biol. Psychiatry *73*, 161–168.

Hennou, S., Kato, A., Schneider, E.M., Lundstrom, K., Gähwiler, B.H., Inokuchi, K., Gerber, U., and Ehrengruber, M.U. (2003). Homer-1a/Vesl-1S enhances hippocampal synaptic transmission. Eur. J. Neurosci. *18*, 811–819.

Hill, M.D., Martin, R.H., Mikulis, D., Wong, J.H., Silver, F.L., Terbrugge, K.G., Milot, G., Clark, W.M., Macdonald, R.L., Kelly, M.E., et al.; ENACT trial investigators (2012). Safety and efficacy of NA-1 in patients with iatrogenic stroke after endovascular aneurysm repair (ENACT): a phase 2, randomised, double-blind, placebo-controlled trial. Lancet Neurol. *11*, 942–950.

Holst, S.C., Sousek, A., Hefti, K., Saberi-Moghadam, S., Buck, A., Ametamey, S.M., Scheidegger, M., Franken, P., Henning, A., Seifritz, E., et al. (2017). Cerebral mGluR5 availability contributes to elevated sleep need and behavioral adjustment after sleep deprivation. eLife *6*, 6.

Hu, J.H., Park, J.M., Park, S., Xiao, B., Dehoff, M.H., Kim, S., Hayashi, T., Schwarz, M.K., Huganir, R.L., Seeburg, P.H., et al. (2010). Homeostatic scaling requires group I mGluR activation mediated by Homer1a. Neuron *68*, 1128–1142.

Hughes, Z.A., Neal, S.J., Smith, D.L., Sukoff Rizzo, S.J., Pulicicchio, C.M., Lotarski, S., Lu, S., Dwyer, J.M., Brennan, J., Olsen, M., et al. (2013). Negative allosteric modulation of metabotropic glutamate receptor 5 results in broad spectrum activity relevant to treatment resistant depression. Neuropharmacology *66*, 202–214.

Inoue, Y., Udo, H., Inokuchi, K., and Sugiyama, H. (2007). Homer1a regulates the activity-induced remodeling of synaptic structures in cultured hippocampal neurons. Neuroscience *150*, 841–852.

Jernigan, C.S., Goswami, D.B., Austin, M.C., Iyo, A.H., Chandran, A., Stockmeier, C.A., and Karolewicz, B. (2011). The mTOR signaling pathway in the prefrontal cortex is compromised in major depressive disorder. Prog. Neuropsychopharmacol. Biol. Psychiatry *35*, 1774–1779.

Kammermeier, P.J., and Worley, P.F. (2007). Homer 1a uncouples metabotropic glutamate receptor 5 from postsynaptic effectors. Proc. Natl. Acad. Sci. USA *104*, 6055–6060.

Kato, A., Ozawa, F., Saitoh, Y., Hirai, K., and Inokuchi, K. (1997). vesl, a gene encoding VASP/Ena family related protein, is upregulated during seizure, long-term potentiation and synaptogenesis. FEBS Lett. *412*, 183–189.

Koike, H., and Chaki, S. (2014). Requirement of AMPA receptor stimulation for the sustained antidepressant activity of ketamine and LY341495 during the forced swim test in rats. Behav. Brain Res. *271*, 111–115.

Krystal, J.H., Mathew, S.J., D'Souza, D.C., Garakani, A., Gunduz-Bruce, H., and Charney, D.S. (2010). Potential psychiatric applications of metabotropic glutamate receptor agonists and antagonists. CNS Drugs *24*, 669–693.

Lee, K.W., Westin, L., Kim, J., Chang, J.C., Oh, Y.S., Amreen, B., Gresack, J., Flajolet, M., Kim, D., Aperia, A., et al. (2015). Alteration by p11 of mGluR5 localization regulates depression-like behaviors. Mol. Psychiatry *20*, 1546–1556.

Li, N., Lee, B., Liu, R.J., Banasr, M., Dwyer, J.M., Iwata, M., Li, X.Y., Aghajanian, G., and Duman, R.S. (2010). mTOR-dependent synapse formation underlies the rapid antidepressant effects of NMDA antagonists. Science *329*, 959–964.

Madisen, L., Zwingman, T.A., Sunkin, S.M., Oh, S.W., Zariwala, H.A., Gu, H., Ng, L.L., Palmiter, R.D., Hawrylycz, M.J., Jones, A.R., et al. (2010). A robust and high-throughput Cre reporting and characterization system for the whole mouse brain. Nat. Neurosci. *13*, 133–140.

Maeng, S., Zarate, C.A., Jr., Du, J., Schloesser, R.J., McCammon, J., Chen, G., and Manji, H.K. (2008). Cellular mechanisms underlying the antidepressant effects of ketamine: role of alpha-amino-3-hydroxy-5-methylisoxazole-4-propionic acid receptors. Biol. Psychiatry *63*, 349–352.

Mansouri, M., Kasugai, Y., Fukazawa, Y., Bertaso, F., Raynaud, F., Perroy, J., Fagni, L., Kaufmann, W.A., Watanabe, M., Shigemoto, R., and Ferraguti, F. (2015). Distinct subsynaptic localization of type 1 metabotropic glutamate receptors at glutamatergic and GABAergic synapses in the rodent cerebellar cortex. Eur. J. Neurosci. *41*, 157–167.

Miller, O.H., Yang, L., Wang, C.C., Hargroder, E.A., Zhang, Y., Delpire, E., and Hall, B.J. (2014). GluN2B-containing NMDA receptors regulate depression-like behavior and are critical for the rapid antidepressant actions of ketamine. eLife *3*, e03581.

Moutin, E., Raynaud, F., Roger, J., Pellegrino, E., Homburger, V., Bertaso, F., Ollendorff, V., Bockaert, J., Fagni, L., and Perroy, J. (2012). Dynamic remodeling of scaffold interactions in dendritic spines controls synaptic excitability. J. Cell Biol. *198*, 251–263.

Mrazek, D.A., Hornberger, J.C., Altar, C.A., and Degtiar, I. (2014). A review of the clinical, economic, and societal burden of treatment-resistant depression: 1996-2013. Psychiatr. Serv. *65*, 977–987.

Nagahara, H., Vocero-Akbani, A.M., Snyder, E.L., Ho, A., Latham, D.G., Lissy, N.A., Becker-Hapak, M., Ezhevsky, S.A., and Dowdy, S.F. (1998). Transduction of full-length TAT fusion proteins into mammalian cells: TAT-p27Kip1 induces cell migration. Nat. Med. *4*, 1449–1452.

Normann, C., Frase, S., Haug, V., von Wolff, G., Clark, K., Münzer, P., Dorner, A., Scholliers, J., Horn, M., Vo Van, T., et al. (2018). Antidepressants rescue stress-induced disruption of synaptic plasticity via serotonin transporter-independent inhibition of L-type calcium channels. Biol. Psychiatry *84*, 55–64.

Nowak, G., Pomierny-Chamioło, L., Siwek, A., Niedzielska, E., Pomierny, B., Pałucha-Poniewiera, A., and Pilc, A. (2014). Prolonged administration of antidepressant drugs leads to increased binding of [(3)H]MPEP to mGlu5 receptors. Neuropharmacology *84*, 46–51.

Okada, D., Ozawa, F., and Inokuchi, K. (2009). Input-specific spine entry of soma-derived Vesl-1S protein conforms to synaptic tagging. Science *324*, 904–909.

Perroy, J., Raynaud, F., Homburger, V., Rousset, M.C., Telley, L., Bockaert, J., and Fagni, L. (2008). Direct interaction enables cross-talk between ionotropic and group I metabotropic glutamate receptors. J. Biol. Chem. *283*, 6799–6805.

Rizzuti, M., Nizzardo, M., Zanetta, C., Ramirez, A., and Corti, S. (2015). Therapeutic applications of the cell-penetrating HIV-1 Tat peptide. Drug Discov. Today *20*, 76–85.

Ronesi, J.A., and Huber, K.M. (2008). Homer interactions are necessary for metabotropic glutamate receptor-induced long-term depression and translational activation. J. Neurosci. *28*, 543–547.

Ronesi, J.A., Collins, K.A., Hays, S.A., Tsai, N.P., Guo, W., Birnbaum, S.G., Hu, J.H., Worley, P.F., Gibson, J.R., and Huber, K.M. (2012). Disrupted Homer

scaffolds mediate abnormal mGluR5 function in a mouse model of fragile X syndrome. Nat. Neurosci. *15*, 431–440, S1.

Schwarze, S.R., Ho, A., Vocero-Akbani, A., and Dowdy, S.F. (1999). In vivo protein transduction: delivery of a biologically active protein into the mouse. Science *285*, 1569–1572.

Serchov, T., Clement, H.W., Schwarz, M.K., Iasevoli, F., Tosh, D.K., Idzko, M., Jacobson, K.A., de Bartolomeis, A., Normann, C., Biber, K., and van Calker, D. (2015). Increased signaling via adenosine A1 receptors, sleep deprivation, imipramine, and ketamine inhibit depressive-like behavior via induction of Homer1a. Neuron *87*, 549–562.

Serchov, T., Heumann, R., van Calker, D., and Biber, K. (2016). Signaling pathways regulating Homer1a expression: implications for antidepressant therapy. Biol. Chem. *397*, 207–214.

Shin, S., Kwon, O., Kang, J.I., Kwon, S., Oh, S., Choi, J., Kim, C.H., and Kim, D.G. (2015). mGluR5 in the nucleus accumbens is critical for promoting resilience to chronic stress. Nat. Neurosci. *18*, 1017–1024.

Sun, P., Wang, F., Wang, L., Zhang, Y., Yamamoto, R., Sugai, T., Zhang, Q., Wang, Z., and Kato, N. (2011). Increase in cortical pyramidal cell excitability accompanies depression-like behavior in mice: a transcranial magnetic stimulation study. J. Neurosci. *31*, 16464–16472.

Ting, J.T., Daigle, T.L., Chen, Q., and Feng, G. (2014). Acute brain slice methods for adult and aging animals: application of targeted patch clamp analysis and optogenetics. Methods Mol. Biol. *1183*, 221–242.

Trivedi, M.H., Rush, A.J., Wisniewski, S.R., Nierenberg, A.A., Warden, D., Ritz, L., Norquist, G., Howland, R.H., Lebowitz, B., McGrath, P.J., et al.; STAR*D Study Team (2006). Evaluation of outcomes with citalopram for depression using measurement-based care in STAR*D: implications for clinical practice. Am. J. Psychiatry *163*, 28–40.

Tronson, N.C., Guzman, Y.F., Guedea, A.L., Huh, K.H., Gao, C., Schwarz, M.K., and Radulovic, J. (2010). Metabotropic glutamate receptor 5/Homer interactions underlie stress effects on fear. Biol. Psychiatry *68*, 1007–1015.

Tu, J.C., Xiao, B., Yuan, J.P., Lanahan, A.A., Leoffert, K., Li, M., Linden, D.J., and Worley, P.F. (1998). Homer binds a novel proline-rich motif and links group 1 metabotropic glutamate receptors with IP3 receptors. Neuron *21*, 717–726.

van Calker, D., Serchov, T., Normann, C., and Biber, K. (2018). Recent insights into antidepressant therapy: Distinct pathways and potential common mechanisms in the treatment of depressive syndromes. Neurosci. Biobehav. Rev. *88*, 63–72.

Xiao, B., Tu, J.C., Petralia, R.S., Yuan, J.P., Doan, A., Breder, C.D., Ruggiero, A., Lanahan, A.A., Wenthold, R.J., and Worley, P.F. (1998). Homer regulates the association of group 1 metabotropic glutamate receptors with multivalent complexes of homer-related, synaptic proteins. Neuron *21*, 707–716.

Xu, J., Zhu, Y., Contractor, A., and Heinemann, S.F. (2009). mGluR5 has a critical role in inhibitory learning. J. Neurosci. *29*, 3676–3684.

Yuen, E.Y., Wei, J., Liu, W., Zhong, P., Li, X., and Yan, Z. (2012). Repeated stress causes cognitive impairment by suppressing glutamate receptor expression and function in prefrontal cortex. Neuron *73*, 962–977.

Zanos, P., Moaddel, R., Morris, P.J., Georgiou, P., Fischell, J., Elmer, G.I., Alkondon, M., Yuan, P., Pribut, H.J., Singh, N.S., et al. (2016). NMDAR inhibition-independent antidepressant actions of ketamine metabolites. Nature *533*, 481–486.

STAR★METHODS

KEY RESOURCES TABLE

REAGENT or RESOURCE	SOURCE	IDENTIFIER
Antibodies		
Rabbit anti-HIV1 TAT (ChiP Grade)	Abcam	Cat# ab43014; RRID: AB_732970
Mouse anti-NeuN	Millipore	Cat# MAB377; RRID: AB_2298772
Rabbit anti-mGlu5	Millipore	Cat# AB5675; RRID: AB_2295173
Rabbit anti-Homer1	Millipore	Cat# ABN37; RRID: AB_11214387
Rabbit anti-phospho-mTOR Ser2448 (D9C2)	Cell Signaling	Cat# 5536; RRID: AB_10691552
Rabbit anti-phospho-p70 S6 Kinase Ser371	Cell Signaling	Cat# 9208; RRID: AB_330990
Rabbit anti-phospho-Akt Ser473	Cell Signaling	Cat# 9271; RRID: AB_329825
Rabbit anti-phospho-Erk1/2 Thr202/Tyr204	Cell Signaling	Cat# 9101; RRID: AB_331646
Rabbit anti-mTOR (7C10)	Cell Signaling	Cat# 2983; RRID: AB_2105622
Rabbit anti-p70 S6 Kinase (49D7)	Cell Signaling	Cat# 2708; RRID: AB_390722
Rabbit anti-Akt	Cell Signaling	Cat# 9272; RRID: AB_329827
Rabbit anti-Erk1/2	Cell Signaling	Cat# 9102; RRID: AB_330744
Rabbit anti-Actin	Sigma-Aldrich	Cat# A5060; RRID: AB_2766001
Mouse anti-CaMKII alpha (Cba-2)	Invitrogen	Cat# 13-7300; RRID: AB_86627
Mouse anti-GluA1-NT (RH95)	Millipore	Cat# MAB2263; RRID: AB_1977459
Rabbit anti-PSD95	Cell Signaling	Cat# 2507; RRID: AB_561221
Rabbit anti-NMDA receptor 2B (D8E10)	Cell Signaling	Cat# 14544; RRID: AB_2798506
Alexa Fluor 488 donkey anti-mouse IgG	Invitrogen	Cat# A-21202; RRID: AB_141607
Alexa Fluor 647 donkey anti-rabbit IgG	Invitrogen	Cat# A-31573; RRID: AB_2536183
Sheep anti-mouse	GE Healthcare	Cat# NA931; RRID: AB_772210
Sheep anti-rabbit	GE Healthcare	Cat# NA9340; RRID: AB_772191
Bacterial and Virus Strains		
BL21(DE3)	NEB	C2527I
rAAV5-hsyn-Homer1a-Venus-WPRE-bGH	Serchov et al., 2015	N/A
rAAV5-hsyn-H1aW24A-Venus-WPRE-bGH	Serchov et al., 2015	N/A
Chemicals, Peptides, and Recombinant Proteins		
4′, 6-diamidino-2-phenylindole	Thermo Fisher Scientific	62248
Mowiol-DABCO	Merck	803456
Imipramine hydrochloride	Sigma-Aldrich	I7379
Ketamine hydrochloride	Pfizer	KETANEST
Metamizole	Zentiva	NOVAMINSULFON
MPEP	Tocris	1212
DHPG	Tocris	0342
Fura-2 AM	Thermo Fisher Scientific	F1201
Anisomycin	Alomone Labs	A-520
NBQX	Tocris	0373
AMPA	Tocris	0169
Tamoxifen	Sigma	T5648
Tetrodotoxin	Alomone Labs	T-550
TAT-mGlu5mut: YGRKKRRQRRR**ALTPPSPFR**	Thermo Fisher Scientific	custom synthesis
TAT-mGlu5act: YGRKKRRQRRR**ALTPLSPRR**	Thermo Fisher Scientific	custom synthesis
TAT-GluA1S845: YGRKKRRQRRR**TLPRNSGAG**	Thermo Fisher Scientific	custom synthesis

(*Continued on next page*)

Continued

REAGENT or RESOURCE	SOURCE	IDENTIFIER
TAT-GluA2$_{3Y}$: YGRKKRRQRRR**YKEGYNVYG**	Thermo Fisher Scientific	custom synthesis
TAT-Scr: YGRKKRRQRRRSTGLAPGRN	Thermo Fisher Scientific	custom synthesis
TAT-Homer1a: MRGS**HHHHHH**GMASMTGGQQMG RDLYDDDDKDRWGSKLG**YGRKKRRQRRR**GGSTM SGYPYDVPDYAGS**MGEQPIFSTRAHVFQIDPNTKK NWVPTSKHAVTVSYFYDSTRNVYRIISLDGSKAIINS TITPNMTFTKTSQKFGQWADSRANTVYGLGFSSEH HLSKFAEKFQEFKEAARLAKEKSQEKMELTSTPSQ ESAGGDLQSPLTPESINGTDDERTPDVTQNSEPRAE PTQNALPFPHRYTFNSAIMIK**	This paper	N/A
TAT-HW24A: MRGS**HHHHHH**GMASMTGGQQMGRDL YDDDDKDRWGSKLG**YGRKKRRQRRR**GGSTMSGYPY DVPDYAGS**MGEQPIFSTRAHVFQIDPNTKKNAVPTSK HAVTVSYFYDSTRNVYRIISLDGSKAIINSTITPNMTFTK TSQKFGQWADSRANTVYGLGFSSEHHLSKFAEKFQEF KEAARLAKEKSQEKMELTSTPSQESAGGDLQSPLTPE SINGTDDERTPDVTQNSEPRAEPTQNALPFPHRYTFN SAIMIK**	This paper	N/A
Critical Commercial Assays		
Ni-NTA Fast Start Kit	QIAGEN	30600
Pierce BCA assay kit	Thermo Fisher Scientific	23225
Pierce ECL Western Blotting Substrate	Thermo Fisher Scientific	32106
M-MLV Reverse Transcriptase	Promega	M1701
iQ SYBR Green Supermix	Bio-Rad	1708880
Experimental Models: Organisms/Strains		
Mouse: Wild type C57BL/6J	Charles River	CEMT Freiburg
Mouse: C57BL/6J-Tg(Thy1-GCaMP6f)GP5.5Dkim/J	Jackson Laboratory	IMSR_JAX: 024276/GP5.5
Mouse: B6;129S6-Tg(Camk2a-cre/ERT2)1Aibs/J	Jackson Laboratory	IMSR_JAX: 012362
Mouse: B6.129-*Grm5*$^{tm1.1Jixu}$/J	Jackson Laboratory	IMSR_JAX: 028626
Oligonucleotides		
qPCR primer Homer1a For: 5‘-CAAACACTGTTTATGGACTG-3‘	Serchov et al., 2015	N/A
qPCR primer Homer1a Rev: 5‘-TGCTGAATTGAATGTGTACC-3‘	Serchov et al., 2015	N/A
qPCR primer Actin For: 5‘-CTAAGGCCAACCGTGAAAAG-3‘	Serchov et al., 2015	N/A
qPCR primer Actin Rev: 5‘-ACCAGAGGCATACAGGGACA-3‘	Serchov et al., 2015	N/A
qPCR primer GAPDH For: 5‘-TGTCCGTCGTGGATCTGAC-3‘	Serchov et al., 2015	N/A
qPCR primer GAPDH Rev: 5‘-CCTGCTTCACCACCTTCTTG-3‘	Serchov et al., 2015	N/A
qPCR primer s12 For: 5‘-GCCCTCATCCACGATGGCCT-3‘	Serchov et al., 2015	N/A
qPCR primer s12 Rev: 5‘-ACAGATGGGCTTGGCGCTTGT-3‘	Serchov et al., 2015	N/A
Accell Green non-targeting control siRNA	Thermo Fisher Scientific	D-001950-01-20
Accell siRNA anti-Homer1a: 5‘-CAGCAATCATGATTAAGTA-3‘	Serchov et al., 2015	Thermo Fisher Scientific

(*Continued on next page*)

Continued

REAGENT or RESOURCE	SOURCE	IDENTIFIER
Recombinant DNA		
pTAT-HA expression vector	Steven Dowdy	Addgene #35612
pTAT-HA-Homer1a	This paper	N/A
pTAT-HA-H1aW24A	This paper	N/A
Software and Algorithms		
FG3xCAP V5.40 video-recording software	HaSoTec	N/A
IntelliCage Plus software	TSE systems	N/A
TILLvisION v4.01 software	TILL Photonics	N/A
Fusion-SL imaging system	Peqlab	N/A
ChemiDoc MP imaging system	BioRad	N/A
VideoMot2 system V6.01	TSE systems	N/A
ImageJ 1.47v software	NIH	N/A
CFX Manager software (Version 3.0.1224.1051, 2012)	Bio-Rad	N/A
ZEN 2.5 software	Carl Zeiss	N/A
GraphPad Prism 8 software	GraphPad Software	N/A

LEAD CONTACT AND MATERIALS AVAILABILITY

Further information and requests for resources and reagents should be directed to and will be fulfilled by the Lead Contact, Tsvetan Serchov (tsvetan.serchov@uniklinik-freiburg.de).

EXPERIMENTAL MODEL AND SUBJECT DETAILS

All procedures were performed in accordance with the German animal protection law (TierSchG), FELASA (http://www.felasa.eu), the guide for care and use of laboratory animals of the national animal welfare body GV SOLAS http://www.gv-solas.de) and the EU Directive 2010/63/EU for animal experiments and were approved by the animal welfare committee of the Universities of Freiburg, Bonn and Bochum as well as by local authorities. Animals were housed in a temperature- and humidity-controlled vivarium and maintained on a 12 h light-dark cycle with *ad libitum* access to food and water. Wild type C57BL/6J mice were obtained from a breeding colony of CEMT-Freiburg. The transgenic mouse line expressing the genetically encoded calcium indicator GCaMP6f under the control of the neuronal Thy1 promoter (Thy1-GCaMP6f) (Dana et al., 2014) was purchased from Jackson Laboratory (C57BL/6J-Tg(Thy1-GCaMP6f)GP5.5Dkim/J; Stock No: 024276/GP5.5). The mouse line with a conditional knockout of mGlu5 selectively in forebrain pyramidal excitatory neurons was generated by crossing CaMK2a-CreERT2 transgenic mice (Jackson Laboratory - B6;129S6-Tg(Camk2a-cre/ERT2)1Aibs/J; Stock No: 012362), that express a tamoxifen-inducible Cre recombinase (CreERT2) under the control of the CaMK2a promoter (Madisen et al., 2010), with a mGlu5floxed line (gift from Anis Contractor), where exon 7 of the mouse Grm5 gene is flanked by loxP sites (Jackson Laboratory - B6.129-*Grm5*$^{tm1.1Jixu}$/J; Stock No: 028626) (Figure 3D) (Xu et al., 2009).

METHODS DETAILS

TAT-Homer1a Fusion Protein Generation, Expression and Purification

To generate TAT-Homer1a fusion proteins a DNA plasmid containing the open reading frame for Homer1a (or its mutated form Homer1aW24A, in which the tryptophan in the ligand binding domain at position 24 is substituted by alanine) was cloned into a pTAT-HA expression vector (gift from Steven Dowdy, Addgene plasmid #35612) to obtain pTAT-HA-Homer1a. The pTAT-HA expression vector carries the T7 bacterial promoter, a polyhistidine (6xHis) tag allowing the purification of the expressed protein, the arginine-enriched cell membrane transduction domain TAT of human immunodeficiency virus 1 (YGRKKRRQRRR) to gain cell permeability (Schwarze et al., 1999) and a hemagglutinin (HA) tag (Nagahara et al., 1998) (Figure 1A). The bacterial expression of TAT-Homer1a/H1aW24 was performed as previously described (Mansouri et al., 2015). The plasmid was transformed into BL21 competent *Escherichia coli* and overnight LB cultures (10 g/L trypton, 5 g/L yeast extract, 5 g/L NaCl, pH 7.2) were induced with 500 μM isopropyl-beta-D-thiogalactopyranoside (IPTG) (Thermo Scientific) for 4 h at 25°C (Becker-Hapak et al., 2001). Fusion proteins were purified under denaturing conditions with the nickel-nitrilotriacetic acid (Ni-NTA) Fast Start Kit (QIAGEN) according to the manufacturer's instructions. Bacteria were sonicated in 8 M urea buffer (pH 8) and centrifuged at 13000 g for 30 min at room temperature. Supernatants were loaded on Ni-NTA columns followed by two washing steps with 8 M urea buffer (pH 6.5) and eluted with 8 M urea buffer (pH 4.5). Denaturing substances were removed from the eluates using PD-10 Desalting Columns (gravity protocol, GE

Healthcare) with 0.9% NaCl as elution buffer. Size and purity of the fusion proteins were verified by sodium dodecyl sulfate–polyacrylamide gel electrophoresis (SDS-PAGE) and western blot and the protein concentration was determined using a bicinchoninic acid (BCA) assay kit (Thermo Scientific) according to the manufacturer's instructions.

Drug Treatment

For acute treatment, mice received a single intraperitoneal (i.p.) injection of ketamine (3 mg/kg ketamine hydrochloride, Pfizer), anisomycin (100 mg/kg dissolved in corn oil, Alomone Labs) or NBQX (10 mg/kg dissolved in saline, Tocris) (Autry et al., 2011) at the indicated time before behavioral testing or sacrifice. To minimize stress during chronic treatment, imipramine (20 mg/kg daily dose, imipramine hydrochloride, Sigma) was given to chronically despaired mice (CDM) via their drinking water for 1 or 4 weeks. For tamoxifen-induced deletion of mGlu5, 8 weeks old CaMK2a-CreERT2*mGlu5floxed mice were i.p. injected with 75 mg/kg tamoxifen (Sigma) dissolved in corn oil once a day over 5 days and behaviorally tested 1 week after treatment (Madisen et al., 2010).

Peptide Administration

TAT-Homer1a fusion proteins and all TAT-peptides (custom-synthetized by Thermo Fisher Scientific) were dissolved in saline and i.v.-injected via the tail vein at the indicated time points before behavioral testing or sacrificing. Dose and route of administration of TAT-Homer1a were chosen as described in Mansouri et al. (Mansouri et al., 2015). The following TAT-peptides were used: TAT-mGlu5act comprising the TAT domain fused to the mGlu5 c-tail EVH1 binding domain for Homer (ALTPPSPFR) and TAT-mGlu5mut – control mutated peptide (ALTP**L**SP**R**R) unable to bind to the Homer EVH1 domain (Ronesi et al., 2012; Ronesi and Huber, 2008; Tronson et al., 2010); TAT-GluA1S845 containing the TAT domain fused to the c-tail S845 PKA phosphorylation site of the AMPA receptor subunit GluA1 (TLPRNSGAG) (Du et al., 2008); TAT-GluA2$_{3Y}$ consists of the TAT domain fused to the c-tail of the AMPA receptor subunit GluA2 containing the 3 tyrosine residues (3Y) (YKEGYNVYG) involved in the regulation of AMPA receptor endocytosis (Brebner et al., 2005; Dalton et al., 2008); TAT-Scr, a TAT domain fused to a scrambled peptide sequence, was used as control.

Behavioral Studies

Activity and behavior of the mice were observed using an automatic video tracking system for recording and analysis (VideoMot2 system V6.01, TSE) and an IntelliCage system (TSE Systems) unless otherwise specified. Open field test, light/dark transition test, elevated plus maze test, tail suspension test, forced swim test and the chronic despair model were performed with male mice. In order to avoid aggressive behaviors only female mice were used for the IntelliCage system experiments (Alboni et al., 2017).

Open Field Test

The test was performed in a square arena (50 × 50 cm) virtually divided into 9 central and 16 peripheral subfields (10 × 10 cm) and surrounded by a 35 cm high wall made of gray PVC. Mice were placed in the center of the field and allowed to move freely. Behavior was recorded for 10 min and total distance traveled and time spent in the central area were analyzed.

Tail Suspension Test

For TST mice were attached with their tails (1–1.5 cm from the tip of the tail) to a horizontal bar located inside a white box (30 × 50 × 20 cm). Each trial was conducted for 6 min and immobility time was determined. Mice observed to climb their tails (> 10% of total time) were eliminated from further analysis.

Forced Swim Test

For the classical FST mice were placed in a transparent glass cylinder (15 cm diameter) filled to a height of 20 cm with water (22-25°C). Immobility time was assessed during a 10 min swim session. Mice were considered to be immobile when they floated in an upright position and made only minimal movements to keep their head above the water.

Light/dark Transition Test

The test apparatus consisted of a box (21 × 42 × 25 cm) divided into a small dark compartment (one third, 5 lux) and a large light compartment (two thirds, 300 lux). Both compartments were connected through a door. Mice were placed into the light compartment and allowed to explore the two chambers for 5 min. Time spent in the light compartment was determined.

Elevated Plus Maze Test

A cross-shaped maze consisting of two open and two closed arms (each 30 × 5 cm) was used for the test. Closed arms were surrounded by a 15 cm high wall. The setup was located 45 cm above the floor and made of gray PVC. Mice were placed in the central open area of the maze facing one of the open arms and observed for 5 min. The time spent in the open and closed arms was assessed.

Chronic Behavioral Despair Model

To induce chronic behavioral despair mice were subjected to repeated swim sessions in a transparent glass cylinder (15 cm diameter) filled to a height of 20 cm with water (22-25°C) 10 min daily for 5 consecutive days (induction phase). After a break of 4 weeks a last swim session was carried out (test phase). In each session the immobility time was recorded and analyzed. The repeated exposure to swimming leads to a chronic (up to 4 weeks) increase of the immobility time and reduction of the sucrose preference during the test phase. The method has been described as a model for depressive-like behavior in mice that allows reliable prediction of antidepressant effects (Figures 1D and 1E and S1G–S1K) (Normann et al., 2018; Serchov et al., 2015; Sun et al., 2011).

Behavioral Analysis in the IntelliCage

The IntelliCage system (TSE Systems) allows simultaneous analysis of spontaneous and exploratory behavior, activity pattern, and drinking preference of up to 16 group-housed mice implanted with radio-frequency identification (RFID) transponders. The unit consists of an open common space with 4 red shelters in the center and 4 recording corners. Mice have free access to food in the middle of the IntelliCage, water is available in the corners behind remote-controlled guillotine doors. Each corner is equipped with 2 drinking bottles and permits the visit of only one mouse at the same time. The scored parameters - the number and duration of visits to any of the 4 corners, the nosepokes toward the doors and the licks on the bottles - were monitored by a PC-based tracking software (IntelliCage Plus, TSE Systems). Initially, the mice were allowed to adapt to the IntelliCage for at least 7 days with water available *ad libitum* in all corners. Then for 3 days the animals were habituated to the sucrose taste: in each corner one of the bottles was filled with 1% sucrose solution and the other one with water. Both doors in the corner were open allowing free choice between the bottles. Next, a nosepoke adaptation period was carried out, where all doors were closed and the mice had to perform a nosepoke to open them. The opened door closes automatically after 5 s of drinking. In all tasks involving sucrose-filled bottles, the positions of the bottles were exchanged every 24ch. The Nosepoke SPT protocol was used (Alboni et al., 2017) for measurement of sucrose preference with gradually increasing effort (number of nosepokes) to reach the sucrose bottles for a short period of time (12 h). In this paradigm each door opens in response to a nosepoke and closes after 5 s licking. The number of nosepokes needed to open a door to a side with a sucrose containing bottle gradually increases (1, 2, 3, 4, 5, 6, 8, 10, 12, 16, 20, 24) after every 8 sucrose licking sessions. For each bottle the number of licks was recorded and the averaged sucrose preference was calculated as percentage of the total number of licks;

Sleep Deprivation

SD was performed using the gentle handling method that includes touching the animals with the hand or a brush and shaking or tapping at the cage. CDM mice were sleep-deprived for 6 h starting at the beginning of the light phase. When indicated, SD was followed by 18 h recovery sleep.

Immunohistochemistry

Animals were anaesthetized with a mix of Ketamin-Rompun (Ketamine [CP Pharma] 50 mg and Rompun [Bayer Healthcare] 0.5 mg per 100 g body weight) and transcardially perfused with 50 mL of ice-cold PBS (8.1 mM Na_2HPO_4, 138 mM NaCl, 2.7 mM KCl and 1.47 mM KH_2PO_4 [pH 7.4]). Brains were removed, postfixed overnight in 4% paraformaldehyde in PBS at 4°C and cryoprotected for 2 days in 30% sucrose in PBS at 4°C. The brains were then frozen and 40 μm coronal sections were cut with a sliding cryostat (Leica Microsystems). Then, the free floating sections were incubated with blocking solution (0.3% Triton X-100 and 5% normal goat serum in PBS) for 1 h at 4°C. Sections were incubated with the respective primary antibody – mouse anti-NeuN (1:1000; Millipore MAB377) and rabbit anti-HIV1 TAT (1:1000; Abcam ab43014) or mouse anti-CaMK2a (1:1000; Invitrogen Cba-2 13-7300) and rabbit anti-mGlu5 (1:1000; Millipore AB5675) - in blocking solution at 4°C overnight. After 3x washing with PBS sections were incubated with the secondary antibodies – Alexa Fluor 488 goat anti-mouse IgG (1:1000; Invitrogen A-21202) and Alexa Fluor 647 donkey anti-rabbit IgG (1:1000; Invitrogen A-31573) - in blocking solution for 3 h at room temperature. Sections were then washed and stained with 1 mg/mL 4,6-diamidino-2-phenylindole (DAPI, 1:1000; Thermo Fisher Scientific 62248) for 10 min. After final washes in PBS slices were mounted on slides using Mowiol-DABCO (Merck 803456). All immunofluorescence images were detected and photographed with a LSM-I-Duo-Live laser scanning confocal microscope and analyzed using ZEN 2.5 software (Carl Zeiss).

In vivo Stereotaxic Microinjections of Recombinant Adeno-Associated Viral Vectors

For stereotaxic injection of recombinant adeno-associated viral vectors (AAV) 1.5 μL of either active AAV-Homer1a or mutated control AAV–H1aW24A (?2 × 1011 particles/mL) were injected bilaterally into the mPFC (anteroposterior +1.4 mm, mediolateral ± 0.6 mm, dorsoventral −2.0 mm, relative to bregma) at a rate of 100 nL/min with a 10 μL syringe fitted with a 34G beveled needle by a microprocessor-controlled minipump (World Precision Instruments) as previously described (Serchov et al., 2015). The mice were sacrificed 4 weeks after the AAV injections.

In vivo Stereotaxic Microinjections of siRNA

For *in vivo* injections endotoxin-free purified FAM-labeled Accell Green non-targeting control siRNA and anti-Homer1a (5'-CAG CAATCATGATTAAGTA-3') Accell siRNA (Thermo Fisher Scientific) were used (Serchov et al., 2015). The mice were isoflurane-anesthetized and placed in a stereotaxic frame. The siRNA (2 μg/μl) dissolved in Accell siRNA delivery media (Thermo Fisher Scientific)

was injected bilaterally with a Hamilton syringe fitted with a 33-gauge needle aimed above the mPFC (anteroposterior +1.34 mm, mediolateral ± 0.6 mm, dorsoventral −2.0 mm, relative to bregma) (Serchov et al., 2015) at a rate of 0.1 μl/min for 5 min (total volume of 0.5 μl/side). The injection needle was briefly left in place and slowly withdrawn (1 mm/min) after the injection. Afterward, animals were allowed to recover from the surgery in individual cages and treated for 24 h with Metamizole (200 mg/kg daily dose) (Zentiva) in the drinking water. The mice were sacrificed 2 days after the injections. The siRNA transfection efficacy and localization were verified by qRT-PCR and immunohistochemistry. *In vivo* application of siHomer1a caused about 40% knockdown efficacy of Homer1a mRNA expression in the mPFC of WT mice, without any significant downregulation in the adjacent cortex and hippocampus and no unspecific effects on the Homer1b/c mRNA levels (Serchov et al., 2015).

Preparation of Acute Brain Slices, *in vitro* Treatment and Fura-2 Calcium Imaging

Acute brain slices were prepared from postnatal day (P) 5-10 C57BL/6J mice. Using a vibratome (T1200, Leica) 300 μm coronal forebrain slices were cut in ice-cold carbogenated artificial cerebrospinal fluid (aCSF) (2 mM NaCl, 2.5 mM KCl, 1.25 mM NaH_2PO_4, 30 mM $NaHCO_3$, 20 mM HEPES, 25 mM glucose, 2 mM $CaCl_2$, 2 mM $MgSO_4$) and recovered for a minimum of 30 min at room temperature. For biochemical analysis the slices were treated for the indicated time periods with the following substances: 100 nM TAT-H1aW24/Homer1a, 5 μM TAT-mGlu5mut/act, 100 nM mGlu1/5 agonist DHPG or 10 μM mGlu5 negative allosteric modulator MPEP.

For calcium imaging the slices were initially incubated with 50 mM Fura-2-acetoxymethyl ester (Invitrogen) in the presence of 1% pluronic acid (Invitrogen) for a maximum of 30 min at 35°C. After a short washing step in aCSF the slices were treated with the respective TAT fusion proteins/peptides for the indicated time periods. Measurements were performed at room temperature in a recording chamber perfused with carbogenated aCSF containing 1 μM tetrodotoxin (Alomone Labs). The NMDA-induced calcium responses were recorded in absence of tetrodotoxin. An upright transmitted light microscope (Axioskop 2 FS Plus, Carl Zeiss) equipped with a 40x water immersion objective (LUMPlan FI/IR, Olympus) and a monochromator (Polychrome IV, TILL Photonics) for excitation were used. With an infrared camera (Imago, TILL Photonics) Fura-2 ratio images (excitation: 340/380 nm, emission 510 nm) were acquired and data were processed using TILLvisION v4.01 software (TILL Photonics). Single Fura-2-fluorescent neurons in the mPFC were selected as regions of interest and the baseline fluorescence signal (F_0) was recorded for at least 30 s before agonist application. The indicated final concentrations of the agonists (DHPG or AMPA, both Tocris Bioscience) were applied in the bath solution followed by wash-out. Images were captured every 250 ms with an exposure time of 20 ms without binning. The pixel brightness ranged between 290-310 (background) and 480-500 (fluorescent neurons) and was shown color-coded on the display. Relative changes in fluorescence were calculated with the formula ($F-F_0/F_0$) where F is fluorescence intensity and F_0 is baseline fluorescence intensity. The area under the curve was determined for 90 s after agonist application. Since we measured the relative change in fluorescence intensity after agonist application ($\Delta F = F - F_0$) with a stable background signal, no background correction was performed. The plotted individual data points represent mean of 15-25 cells per slice.

Calcium Imaging with Thy1-GCaMP6f Mice

To prepare acute slices adult 8-12 weeks old Thy1-GCaMP6f mice were sacrificed by cervical dislocation after 10 min oxygenation. Using a vibratome (T1200, Leica) 300 μm coronal slices containing mPFC were cut in ice-cold carbogenated N-methyl-D-glucamine (NMDG) aCSF (92 mM NMDG, 2.5 mM KCl, 1.25 mM NaH_2PO_4, 30 mM $NaHCO_3$, 20 mM HEPES, 25 mM glucose, 2 mM thiourea, 5 mM sodium ascorbate, 3 mM sodium pyruvate, pH 7.3–7.4, 0.5 mM $CaCl_2$, 10 mM $MgSO_4$). For recovery slices were first incubated in carbogenated NMDG aCSF (32-34°C) for 10 min and afterward in carbogenated holding aCSF (2 mM NaCl, 2.5 mM KCl, 1.25 mM NaH_2PO_4, 30 mM $NaHCO_3$, 20 mM HEPES, 25 mM glucose, 2 mM thiourea, 5 mM sodium ascorbate, 3 mM sodium pyruvate, 2 mM $CaCl_2$, 2 mM $MgSO_4$) at room temperature for a minimum of 30 min. (Ting et al., 2014). The measurements were performed as described above. GCaMP6f fluorescence images were acquired at an emission wavelength of 505-530 nm using 470 nm for excitation. The area under the curve was calculated for 30 s (DHPG) or 60 s (AMPA) after agonist application.

Preparation of Total, Synaptosomal and PSD Fractions

Dissected brain regions or the whole acute slices were mechanically homogenized in either homogenization buffer (320 mM sucrose, 4 mM HEPES [pH 7.4], 2 mM EDTA) or immunoprecipitation (IP) buffer (50 mM Tris HCl [pH 7.4], 120 mM NaCl, 5 mM EDTA, 0.5% Triton X-100) and centrifuged at 800 g for 10 min at 4°C to generate total (S1) and nuclear fraction (P1). All buffers contained a phosphatase and protease inhibitor cocktail (Sigma-Aldrich). Synaptic (P2) and cytosolic (S2) fractions were obtained by centrifugation of S1 at 10 000 g for 20 min at 4°C. Washed synaptosomal pellets (P2) were either processed for PSD isolation or directly lysed in lysis buffer (50 mM Tris-HCl [pH 6.8], 1.3% SDS, 6.5%, glycerol, 100 μM sodium orthovanadate) containing phosphatase and protease inhibitor cocktail (Sigma-Aldrich) and boiled for 10 min at 95°C and processed for SDS-PAGE and western blot. For PSD isolation P2 was resuspended in 4 mM HEPES [pH 7.4] and 2 mM EDTA, incubated for 30 min at 4°C and centrifugated at 25 000 g for 20 min at 4°C. Obtained pellets were resuspended in homogenization buffer, placed on top of sucrose gradient (0.8 M, 1.0 M and 1.2 M sucrose with 4 mM HEPES [pH 7.4] and 2 mM EDTA) and centrifuged at 150 000 g for 2 h at 4°C. The collected fraction at the interface between 1.0 M and 1.2 M was pelleted by centrifugation at 150 000 g for 30 min at 4°C, lysed in lyse buffer and processed for SDS-PAGE and western blot. The protein concentration of the different fractions was determined using a BCA assay kit (Thermo Fisher Scientific) according to the manufacturer's instructions.

Co-immunoprecipitation

350 μg protein from total lysate was immunoprecipitated with 1 μg rabbit anti-mGlu5 antibody (Millipore, AB5675) overnight at 4°C followed by 1 h incubation with 50 μl Protein A/G PLUS-agarose beads (Santa Cruz Biotechnology) at 4°C. After three washing steps with IP buffer bound proteins were eluted with lysis buffer, containing 10 mM dithiothreitol (DTT) and bromphenol blue, boiled for 10 min at 95°C and analyzed by SDS-PAGE and western blot.

Western Blot

After adding 10 mM DTT and bromphenol blue total (S1) (mixed 1:1 with lysis buffer) or synaptosomal (P2) lysates were boiled for 10 min at 95°C, separated by SDS-PAGE on 7.5% - 12% acrylamide gels and transferred to polyvinylidene difluoride (PVDF) membranes (Merck Millipore). The membranes were blocked with 5% non-fat dry milk in TBS-T (1% Tween20 in Tris-buffered saline (TBS)) or Roti-Block (Carl Roth) and afterward incubated with the respective primary antibodies diluted in TBS (rabbit anti-mGlu5, Millipore (AB5675), 1:2000; mouse anti-GluA1-NT, Millipore (MAB2263), 1:1000; rabbit anti-NMDA receptor 2B (D8E10), Cell Signaling (14544), 1:1000; rabbit anti-Actin, Sigma-Aldrich (A5060), 1:1000; rabbit anti-PSD95, Cell Signaling (2507), 1:2000; mouse anti-PSD95, Thermo Scientific (7E3-1B8), 1:2000; rabbit anti-Homer1, Millipore (ABN37), 1:1000; mouse anti-HA tag BioLegend (90150), 1:1000; rabbit anti-phospho-mTOR Ser2448, Cell Signaling (5536), 1:1000; rabbit anti-phospho-p70 S6K Ser371, Cell Signaling (9208), 1:500; rabbit anti-phospho-Akt Ser473, Cell Signaling (9271), 1:500; rabbit anti-phospho-Erk1/2 Thr202/Tyr204, Cell Signaling (9101), 1:1000; rabbit anti-mTOR, Cell Signaling (2983), 1:1000; rabbit anti-p70 S6 Kinase, Cell Signaling (2708), 1:1000; rabbit anti-Akt, Cell Signaling (9272), 1:1000; rabbit anti-Erk1/2, Cell Signaling (9102), 1:1000) overnight at 4°C. After 3 times washing membranes were incubated with horseradish peroxidase-conjugated secondary antibodies diluted in TBS-T (sheep anti-mouse, GE Healthcare (NA931), 1:20000; donkey anti-rabbit, GE Healthcare (NA9340), 1:25000) for 1 h at room temperature. Washed membranes were developed with either a Fusion-SL imaging system (Peqlab) or a ChemiDoc MP imaging system (Bio-Rad) using enhanced chemiluminescence detection kit (Thermo Fisher Scientific). Band intensity was quantified by densitometry with ImageJ 1.47v software (National Institute of Health, USA) and normalized to the appropriate loading control.

Quantitative Real-time PCR (qRT-PCR)

Mice from each experimental group were killed by cervical dislocation. The brain was rapidly removed and the medial prefrontal cortex was dissected and quickly frozen on dry ice and stored at −80°C until used for RNA isolation. The RNA extraction and expression analyses were performed as previously described (Serchov et al., 2015). Briefly, the tissues were homogenized in guanidine thiocyanate/2-mercaptoethanol buffer and total RNA was extracted with the sodium acetate/phenol/chloroform/isoamylacohol procedure. Then, samples were isopropanol-precipitated and washed twice with 70% ethanol. The pellets were dissolved in RNase-free Tris-HCl buffer (pH 7.0) and RNA concentrations were determined with a spectrophotometer (BioPhotometer; Eppendorf). Reverse transcription was performed with 1 mg of total RNA using M-MLV reverse transcriptase (Promega). The quantitative real-time PCR was done on a C1000TM Thermal Cycler (CFX96 real-time PCR system, Bio-Rad) using iQ SYBR Green Supermix (BioRad). All qRT-PCR experiments were performed blinded as the coded cDNA samples were pipetted by a technician. The target gene mRNA levels were normalized to the levels of actin, glyceraldehydes-3-phosphate dehydrogenase (GAPDH) and s12 RNA automatically by CFX Manager software (Version 3.0.1224.1051, 2012, Bio-Rad) using the ''Gene study'' option via geometric averaging of multiple internal control genes. The primer sequences used were as follows - Homer1a: 5'-CAAACACTGTTTATGGACTG-3', 5'-TGCTGAATTGAATGTG TACC-3'; actin: 5'-CTAAGGCCAACCGTGAAAAG-3', 5'-ACCAGAGGCATACAGGGACA-3'; GAPDH: 5'-TGTCCGTCGTGGATCT GAC-3', 5'-CCTGCTTCACCACCTTCTTG-3'; s12: 5'-GCCCTCATCCACGATGGCCT-3', 5'-ACAGATGGGCTTGGCGCTTGT-3'.

Statistical Analysis

All values are expressed as means ± SEM. Statistical analyses were performed with GraphPad Prism 8.0.0 software (GraphPad Software) using one- or two-way analysis of variance (ANOVA) followed by Bonferroni post hoc test to compare the means of two or more groups or unpaired two-tailed Student's t test to compare the means of two groups. A p value ≤ 0.05 was considered to be significant (*$p \leq 0.05$, **$p \leq 0.01$, ***$p \leq 0.001$). Detailed statistical approaches and results are provided in Table S1, statistical analysis summaries are mentioned in the figure legends. Prior to statistical analyses data assumptions (for example normality and homoscedasticity of the distributions) were verified using Anderson-Darling, D'Agostino-Pearson, Shapiro-Wilk and Kolmogorov-Smirnov tests (GraphPad Prism 8.0.0 software). For all molecular and behavioral studies mice were randomly assigned to the groups. Most behavioral and molecular results were confirmed via independent replication of the experiments as shown in Table S1. Additionally, investigators were blinded to the treatment group until data have been collected. Sample sizes were determined on the basis of extensive laboratory experience and were verified via power analysis.

DATA AND CODE AVAILABILITY

The datasets generated and/or analyzed during the current study are available from the lead contact and corresponding author (Dr. Tsvetan Serchov) on reasonable request.